UNIVERSITY OF CALIFORNIA, SAN DIEGO

Control of Circadian and Reproductive Behavior and Physiology

A dissertation submitted in partial satisfaction of the requirements for the degree of Doctor of Philosophy

in

Biology

by

Daniel D. Clark

Committee in Charge:

Professor Pamela L. Mellon, Chair
Professor Nicolas S. Spitzer, Co-Chair
Professor Mark A. Lawson
Professor Cornelis Murre
Professor Satchidananda Panda
Professor David K. Welsh

2011

The Dissertation of Daniel D. Clark is approved, and it is acceptable in quality and form for publication on microfilm and electronically:

_____

_____

_____

_____

_____
Co-Chair

_____
Chair

University of California, San Diego

2011

Dedication

This dissertation
is dedicated
to Lindz

Epigraph

Wonder is the beginning of wisdom.
-Socrates

Table of Contents

List of Abbreviations and Symbols

ARC	Arcuate nucleus
AVP	Arginine vasopressin
AVPV	Anteroventral periventricular nucleus
CP	Cribriform plate
GnRH	Gonadotropin-releasing hormone
e	Embryonic day of age
FSH	Follicle-stimulating hormone
HPG	Hypothalamic pituitary gonadal
KO	Knock-out
LH	Luteinizing hormone
ME	Median eminence
OCh	Optic chiasm
ON	Optic nerve
OVLT	Organum vasculosum of lamina terminalis
p	Post-natal day of age
RHT	Retinohypothalamic tract
SCN	Suprachiasmatic nucleus
τ	Tau, period of circadian rhythmicity
VIP	Vasoactive intestinal polypeptide
V.O.	Vaginal opening
WT	Wild-type

List of Figures

List of Tables

Acknowledgements

Without the following people (in approximate chronological order), the completion of this dissertation would not have been possible: Chris Colwell and Stephan Michel (UCLA), Jean-Pyo Lee and Evan Snyder (Burnham), Bill Kristan and Kathy French (neuroscience boot camp, graduate rotations), Nick Spitzer and Satchin Panda (graduate rotations, committee membership), Pamela Mellon (advisor, mentor), Bruce Hamilton (genetics training grant), Mark Lawson, Cornelis Murre, and David Welsh (committee membership, advice), Michael Gorman (advice, co-authorship), and Lara Kose (master's student). I would also like to thank Pat, Sara, Alex, Nichol, Rae, Kina, Djurdjica, Kellie, Natalie, Susan, Melissa, Kristal, Em, Emily, Baymate Anita, Christine, Lacey, Arpi, Huimin, Paul, Raj, De'Nise, Peeps, Azim, Sheila, Matt, Polly, Hanne, Ikuo, Scholar Johnson, Scholar Takimoto, Scholar Ulin, Scholar Shirley, Scholar Egan, Scholar Dekelver, Scholar Koehler, Shandog, Jules, Lindsay, Bari, Rebecca, Klagor, Jeff, Derek, Ben, Angela, Adam, and everyone else who has helped and encouraged me at UCSD.

Chapter 1 is a reprint of material appearing in the Journal of Neuroscience 2011. Larder, Rachel; Clark, Daniel; Miller, Nichol; Mellon, Pamela. "Hypothalamic Dysregulation and Infertility in Mice Lacking the Homeodomain Protein Six6." Journal of Neuroscience, 2011 Jan 12; 31(2):426-38. This paper was written by Rachel Larder; the dissertation author was the second author of this paper.

Material from Chapter 2 has been submitted for publication in the Journal of Biological Rhythms. Clark, Daniel D.; Gorman, Michael R.; Mellon, Pamela L. "The Homeodomain Protein Six6 is Required for Development of the Suprachiasmatic Nucleus and Circadian Rhythms."

Vita

2002	Bachelor of Science, University of California, Los Angles
2002-2005	Research Assistant, The Burnham Institute
2010	Instructor of Record, BIMM 101, Recombinant DNA Techniques
2011	Doctor of Philosophy, University of California, San Diego

Publications

The Homeodomain Protein Six6 is Required for Development of the Suprachiasmatic Nucleus and Circadian Rhythms. Daniel D. Clark, Michael R. Gorman, Pamela L. Mellon. Submitted to the Journal of Biological Rhythms.

Hypothalamic Dysregulation and Infertility in Mice Lacking the Homeodomain Protein Six6. Larder R, Clark DD, Miller N, Mellon PL. The Journal of Neuroscience, January 12, 2011, 31(2):426-438.

Fertility Effects of Tissue-Specific Bmal Inactivation. Clark D, Mellon P. Gordon Research Conference, Chronobiology. Salve Regina University, July 19-24, 2009. [Poster Abstract]

GnRH Neuron Locations and Projections in the Hypogonadotropic Hypogonadal Mouse. Clark DD, Miller NLG, Mellon PL. The Endocrine Society's 89th Annual Meeting. Toronto, June 2-5, 2007. [Poster Abstract]

Stem cells act through multiple mechanisms to benefit mice with neurodegenerative metabolic disease. Lee JP, Jeyakumar M, Gonzalez R, Takahashi H, Lee PJ, Baek RC, Clark D, Rose H, Fu G, Clarke J, McKercher S, Meerloo J, Muller FJ, Park KI, Butters TD, Dwek RA, Schwartz P, Tong G, Wenger D, Lipton SA, Seyfried TN, Platt FM, Snyder EY. Nature Medicine. 2007 Apr;13(4):439-47.

Neural Stem Cell Therapy in Lysosomal Storage Disease. Jean-Pyo Lee, Dan Clark, Mylvaganam Jeyakumar, Rodolfo Gonzalez, Scott McKercher, Franz-Josef Mueller, Rahul Jandia, Rosanne M. Taylor, Kook In Park, Thomas N. Seyfried, Frances M. Platt & Evan Y. Snyder. Chapter in Lysosomal Storage Disorders. Edited by John A. Barranger and Mario A. Cabrera-Salazar. Springer US, 2008. ISBN: 978-0-387-70908-6.

ABSTRACT OF THE DISSERTATION

Control of Circadian and Reproductive Behavior and Physiology

by

Daniel D. Clark

Doctor of Philosophy in Biology

University of California, San Diego, 2011

Professor Pamela L. Mellon, Chair
Professor Nicolas S. Spitzer, Co-Chair

Mammalian reproduction is mediated by the hypothalamic-pituitary-gonadal axis. The gonadotropin-releasing hormone (GnRH) neuron is the final central output of the hypothalamic portion of this axis, and the proper development and function of this neuronal type is required for normal fertility. Several genes have been identified as necessary for GnRH neuron development and function, including the homeodomain protein *Six6*, a homologue of *Drosophila optix*.

Mice lacking the *Six6* gene have several previously identified phenotypes—predominantly phenotypes of the eye and retina—and additional phenotypes are described here. Male and female *Six6*-/- mice have impaired fertility due, in part, to

significantly reduced numbers of GnRH neurons relative to wild-type littermate control animals.

Additional phenotypes identified in the *Six6*-/- mice were circadian- and suprachiasmatic nucleus- (SCN-) related. *Six6*-/- mice displayed a variety of circadian behavioral activity patterns, with some mice showing periodicity during constant darkness, and other mice completely lacking circadian periodicity even in entrainment photoperiods. However, regardless of behavioral phenotype or the previously identified optic nerve phenotype, *Six6*-/- mice lacked suprachiasmatic nuclei as indicated by immunostaining for prototypical SCN markers and observation of hypothalamic morphology.

The circadian clock controls many aspects of mammalian physiology, including reproduction in many species. Inactivation of the circadian clock in mice, via knock-out of *Bmal* leads to infertility, though the mechanisms underlying this infertility remained incompletely understood. Using transgenic, physiological, and behavioral techniques, the reproductive phenotype of *Bmal*-/- mice was investigated. Tissue-specific inactivation of *Bmal* in all neurons or in GnRH neurons did not appreciably affect fertility, though neuronal *Bmal* inactivation resulted in a shortening of the free-running circadian period. Female *Bmal*-/- mice were unable to respond to estrogen stimulation with an appropriate LH surge. Male *Bmal*-/- mice showed severely impaired mating behavior, and even *Bmal*-/- mice given testosterone replacement exogenously did not show normal mating behavior.

Introduction

The Earth rotates about its axis every 24 hours and orbits the sun with a period of approximately one year. Nearly every organism on the planet has adapted to the resultant daily and yearly changes in environmental conditions. The field of chronobiology studies the physiological changes life undergoes in anticipation and response to these periodic changes in the environment. One key component of these physiological changes, in many organisms, is the circadian clock (from the Latin: “circa” meaning “approximately” and “dia” meaning “day”). Because the duration of daylight waxes and wanes yearly, the circadian clock of many organisms tracks not only the daily light/dark cycle, but also the yearly seasons.

The adaptive importance of the circadian clock is reflected in the diverse domains of physiology it exerts control over—even in the absence of external environmental cues for actual time of day. The circadian clock in many plants allows them to anticipate dawn—the cellular photosynthetic machinery (Dodd, 2005) [and even the physical orientation of the plant itself, in some cases (Niinuma, 2005)] is primed for activity prior to sunrise. The digestive system of many mammalian species is directed to be most active during periods of the day during which food will be available (Challet, 2010). The sleep-wake cycle is acutely regulated by the circadian clock, with nocturnal animals quiescent during the day and diurnal animals active during the daylight hours.

The influence that the circadian system has over reproduction is another physiological output of the clock—and is the topic of this dissertation. Seasonal breeders with diverse gestation periods time conception such that birth occurs in a season of the year most likely to result in the survival of their offspring (Goldman,

1999; Lincoln, 1981). In these animals, the length of daylight signals to and entrains the circadian clock so that it can direct the appropriate physiological changes in the reproductive system. In non-seasonal breeders such as rodents, the circadian clock's influence is less profound, but no less important. In mice, the timing of daily reproductive hormonal (reproductive neuroendocrine) changes—controlled by the circadian clock—provide a window of time (Bronson, 1979) during which females are fertile: their period of highest activity and likeliest chance of finding a mate.

The central component of the mammalian circadian clock—the suprachiasmatic nucleus, or SCN—is a brain structure in the region of the hypothalamus (Turek, 1996). Surgical ablation of this nucleus abolishes circadian rhythms of physiology, including behavior, metabolism, and reproduction. In addition to abolishing the circadian components of reproduction such as daily fluctuations in hormones, SCN ablation in mice also results in infertility.

Within the cells of the SCN—indeed, within most cells in the body of most mammals—the basis for the 24 hour rhythms is a timed program of gene transcription and translation. Several interacting transcription-translation loops have been identified in this program and are here described briefly for the case of mammals—though similar programs with homologous players can be found from plants through flies. The transcription factors Clock and Bmal heterodimerize to form an activating transcriptional unit that activates many genes including the *Period* (*Per*) and *Cryptochrome* (*Cry*) genes. Per and Cry are translated, are post-translationally modified, and then translocate into the nucleus. The Per and Cry dimers and heterodimers then transcriptionally silence their own genes by binding to Clock and Bmal and sequestering them off the DNA. This forms the basis for the "core"

transcription-translation loop of the cellular clock program. Another important loop involves the genes for Ror-α and Ror-β and Rev-erb-α and Rev-erb-β activating (Ror) or inactivating (Rev-erb) *Bmal* transcription (Ueda, 2005).

Most of these clock genes were originally identified through genetic manipulations and the study of these mutant or knock-out mice provide key insights into the role the circadian clock plays in reproduction (Boden, 2006). The reproductive consequences of genomic clock gene inactivation include lack of an LH surge and increased rates of embryo resorption and difficulties in the $Clock^{\Delta 19}$ mutant mouse (Miller, 2004), and the problems with gestation in $Clock^{\Delta 19}$ mutant females persisted or worsened when the animals were kept in constant darkness (Dolatshad, 2006).

Key among the circadian transgenic or mutant mice, however, is the *Bmal* knock-out mouse. Knock-out of *Bmal* leads to complete arrhythmia in constant darkness, with weak if any oscillatory ultradian rhythmicity (Bunger, 2000). *Bmal* knock-out mice were originally reported to be fertile (Cowden, 2002), however subsequent work—beginning with two early abstracts noting impaired fertility (**Boden**, 2004; Boden, 2005)—revealed that this was not the case. Female *Bmal*-/- fertility defects include prolonged (Ratajczak, 2009) or variably prolonged or acyclic (Boden, 2010) estrous cycles and a failure of embryo implantation due to low serum progesterone concentrations (Ratajczak, 2009). Male *Bmal*-/- fertility defects include impairment of testis function and decreased expression of the steroidogenesis rate-limiting gene *steroidogenic acute regulatory protein* (*StAR*) (Alvarez, 2008).

Mammalian reproduction is physiologically controlled by a neuroendocrine axis (the HPG axis) comprised of the hypothalamus, the pituitary, and the gonads. A small population of cells diffusely localized throughout the hypothalamus produce the

neuropeptide gonadotropin-releasing hormone (GnRH). Axons of these GnRH neurons project to and terminate in a structure called the median eminence. GnRH secreted from the median eminence enters a specialized system of blood vessels—the hypophyseal portal system (from the Latin “hypophesis” meaning “pituitary”)—where portal blood conveys GnRH to cells in the anterior pituitary. Gonadotrope cells here express the receptor for GnRH and respond to GnRH stimulation by secreting the gonadotropins luteinizing hormone (LH) and follicle-stimulating hormone (FSH) into the peripheral bloodstream. Receptors for LH and FSH exist in cells of the gonad, either the ovarian granulosa and theca cells or the testicular Leydig and Sertoli cells. The gonads—in response to the gonadotropin signaling—carry out the physiology of reproduction from steriodogenesis to ovarian follicle maturation, ovulation, and sperm maturation. The gonadal steroids then enter the peripheral bloodstream from whence they can signal back to the hypothalamus and pituitary, completing the HPG axis feedback loop.

The GnRH neurons at the apex of the HPG axis are one primary topic of investigation in my lab. Two of the tools we use to investigate GnRH neuron function are model cell lines that represent GnRH neurons at different stages of development. The GT1-7 cell line (Mellon, 1990) represents mature, terminally differentiated GnRH neurons, while the GN11 cell line (Radovick, 1991) represents immature, migratory GnRH neurons. By comparing the gene expression profiles of these two cell lines, we can infer likely changes in gene expression that take place *in vivo* in GnRH neurons during their development and maturation. Several highly differentially regulated genes have been identified between the GT1-7 and GN11 cells, including the *GnRH* gene itself.

Another of the most differentially regulated genes in GnRH neurons was the homeodomain transcription factor *Six6*. This gene was known to play an important role in eye and retina development, and is a homologue of the *Drosophila optix* gene (Jean, 1999). However, given its striking degree of differential regulation (nearly to the degree of the *GnRH* gene itself), we wanted to characterize its role in reproduction. The *Six6* knock-out mouse had already been created to study the role *Six6* plays in eye development, and we obtained this knock-out mouse for study of its reproduction.

The study of these two knock-out mice forms the basis of the research presented in this dissertation. The *Six6* knock-out mice were originally identified in our lab to have profound reproductive deficits (Chapter 1; written by Rachel Larder, with experimental and data analysis contributions from the dissertation author) and we later identified profound defects in circadian rhythmicity (Chapter 2). The *Bmal* knock-out mice (Chapter 3) bear a genetic defect intended to abolish circadian rhythmicity and we identified and characterized profound reproductive deficits.

Chapter 1: Hypothalamic Dysregulation and Infertility in Mice Lacking the Homeodomain Protein Six6

Chapter 1.1: Introduction

Mammalian reproduction is mediated by the pulsatile release of gonadotropin-releasing hormone (GnRH) from a distinct population of neurons within the hypothalamus. GnRH stimulates the anterior pituitary gland to secrete gonadotropins, which, in turn, act on the gonads to control gametogenesis. GnRH neurons have a unique point of origin within the olfactory placode (OP) at embryonic day (e) 11.5 (Schwanzel-Fukuda, 1992; Schwanzel-Fukuda, 1989; Wray, 1989). From the OP, they migrate across the cribriform plate and through the basal forebrain to arrive within the presumptive hypothalamus by e17.5. They then extend their axons to the median eminence to allow secretion of GnRH into the hypophyseal portal system.

Since adult mice have only ~800-1000 GnRH neurons, dispersed throughout the septohypothalamic region (Wray, 1989), analysis of GnRH transcriptional regulation has benefited from the generation of immortalized cell lines (Mellon, 1990; Radovick, 1991). GT1-7 cells represent a fully differentiated GnRH neuron that secretes high levels of GnRH in a pulsatile manner (Wetsel, 1991; Wetsel, 1992). In contrast, GN11 cells represent a developmentally earlier, migratory GnRH neuron that expresses low levels of GnRH and responds to migratory cues (Radovick, 1991). Using these cell lines, enhancer and promoter elements have been characterized (Givens, 2004; Iyer, 2010; Kim, 2007; Kim, 2002; Lawson, 2002) and several transcription factors that regulate GnRH gene expression have been elucidated (Clark, 1995; Fang, 1998; Kelley, 2000; Larder, 2009; Lawson, 1996; Pierce, 2008; Rave-Harel, 2004; Rave-Harel, 2005; Wierman, 1997; Wolfe, 2002).

Recently we reported necdin, a Prader-Willi syndrome candidate gene, as the most differentially expressed transcript from a comparative microarray screen of GN11 and GT1-7 cell mRNA (Miller, 2009). We identified a further ~2000 transcripts that were significantly up-regulated in the more mature GT1-7 cell line (unpublished observations). One of the most differentially expressed transcripts corresponded to Six6, a homeodomain protein and vertebrate homologue of *Drosophila optix* (Jean, 1999). Mammalian Six proteins have two highly conserved domains; a homeodomain and a 'Six' domain and are classified into three subfamilies based on the homology of these domains (Seo, 1999). While Six1, Six2, Six4, and Six5 all show broad expression during embryogenesis, Six3 and Six6 are restricted to the developing eye and brain (Jean, 1999; Oliver, 1995). However, despite their initial overlapping pattern, their expression becomes segregated in the postnatal brain, with Six6 expression becoming confined to the adult hypothalamus (Conte, 2005). With our identification of Six6 as one of the most up-regulated genes in the GT1-7 cells as compared to the GN11, we sought to determine its role in the control of GnRH neuronal maturation and its contribution to fertility *in vivo*.

Chapter 1.2: Materials and Methods

Microarray data analysis and PCR. Extraction of RNA for microarray experiments and analysis of microarray data was performed as previously described (Miller, 2009). Adult mouse hypothalamus, pituitary, testes, ovary, and eye cDNA were purchased from Zyagen. Preparation of cDNA from cultured cells and RT-PCR were performed as previously described (Larder, 2004). Standard PCR conditions were used and were identical for all primers. Quantitative RT-PCR (Q-RT-PCR)

amplification utilized GN11 or GT1-7 cDNA, IQ SYBR Green Supermix (Bio-Rad), specific primer sequences (Table 1.1) and an IQ5 Real-time PCR instrument (Bio-Rad). Q-RT-PCR was performed as previously described (Larder, 2009).

Table 1.1. Sequences of oligonucleotides. Mutated sequences are underlined; bp, base pairs.

Primers	DNA Sequence
RT-PCR Six6 Forward RT-PCR Six6 Reverse	5’ TCGATGTTCCAGCTGCCCAT 3’ 5’ TGGAAAGCCACGATGGCTCT 3’
RT-PCR Six3 Forward RT-PCR Six3 Reverse	5’ CCACTGCTCCCTACTTCTGG 3’ 5’ GCAACTGGAACATGGACAAC 3’
RT-PCR GapDH Forward RT-PCR GapDH Reverse	5’ ATGGGTGAAGGTCGGTGTGA 3’ 5’ GCTTCCCGTTGATGACAAGC 3’
Q-RT-PCR Six6 Forward Q-RT-PCR Six6 Reverse	5’ GCATTACCAGGAGGCAGAGA 3’ 5’ GGGATATGGGTCCTGAAGGT 3’
Q-RT-PCR Six3 Forward Q-RT-PCR Six3 Reverse	5’ CCGGAAGAGTTGTCCATGTT 3’ 5’ CGACTCGTGTTTGTTGATGG 3’
Q-RT-PCR GnRH Forward Q-RT-PCR GnRH Reverse	5’ TGCTGACTGTGTGTTTGGAAGGCT 3’ 5’ TTTGATCCACCTCCTTGCGACTCA 3’
Q-RT-PCR GapDH Forward Q-RT-PCR GapDH Reverse	5’ TGCACCACCAACTGCTTAG 3’ 5’ GGATGCAGGGATGATGTTC 3’
-41 bp EMSA Forward -41 bp EMSA Reverse	5’ CATTCCTCATTAAATGGCTTTTTGT 3’ 5’ ACAAAAAGCCATTTAATGAGGAATG 3’
-53 bp EMSA Forward -53 bp EMSA Reverse	5’ CAGGTGTTCCAATTACATTCCTCAT 3’ 5’ ATGAGGAATGTAATTGGAACACCTG 3’
-1622 bp EMSA Forward -1622 bp EMSA Reverse	5’ TATAAAGCCCAATTACTTAAACCCA 3’ 5’ TGGGTTTAAGTAATTGGGCTTTATA 3’
-1635 bp EMSA Forward -1635 bp EMSA Reverse	5’ AAAATTGTGACAATTATAAAGCCCA 3’ 5’ TGGGCTTTATAATTGTCACAATTTT 3’
Six3 DelN Mutant Forward Six3DelN Mutant Reverse	5’ TGGATGTTCCAGTTGCCCAC 3’ 5’ ATCATACATCACATTCCGAG 3’
E Del Mutant Forward E Del Mutant Reverse	5’ GAAAATTGTGATAAAGCCCTTAAACCCAA 3’ 5’ GACAAATTGGGTTTAAGGGCTTTATCACA 3’
P Del Mutant Forward P Del Mutant Reverse	5’ GACCAGCAGGTGTTCCATTCCTAATGGCT 3’ 5’ TCACAAAAAGCCATTAGGAATGGAACACC 3’
Six6 Genotyping Forward Six6 Genotyping WT Reverse Six6 Genotyping KO Reverse	5’ AAGACAGACTGCATTCCCAGCTCCC 3’ 5’ AGACTCACTGCTTCAAGGAGCGCAC 3’ 5’ AGCCTGAAGAACGAGATCAGCAGCC 3’

Mouse breeding and genotyping. Mouse colonies were maintained in agreement with protocols approved by the Institutional Animal Care and Use Committee at the University of California, San Diego. All animals were housed under a 12 h light-dark cycle and provided with food and water *ad libitum*. Six6-null mice were generated as previously described (Li, 2002) and were kindly provided by Dr. Xue Li (Children's Hospital of Boston, Harvard Medical School, Boston). All mice were on a mixed 129/Sv and C57BL/6J genetic background.

Determination of day of vaginal opening and phase of estrous cycle. After weaning (20 days), all female mice were inspected daily and the age at vaginal opening recorded. To assess estrous cyclicity, vaginal smears were obtained from 4-6 month old mice by vaginal lavage, over a period of at least 21 continuous days. Vaginal lavage was performed daily (at 10 am) by flushing the vagina with distilled H_2O. Collected smears were mounted on glass slides and examined microscopically for cell type (Becker, 1995).

Vaginal plug formation. To monitor plug formation, a fertile C57BL/6J female mouse was housed with either a wild-type, heterozygous or homozygous Six6-null male (8-12 weeks of age). The following morning, females were checked for the presence of vaginal plugs. If a plug was present, the female was removed to a separate cage. If no plug was detected, the female remained in the cage with the male. Plug checks were performed for 10 consecutive days.

Fertility assessment and hormone measurements. At 8 weeks of age, wild-type, heterozygous or homozygous Six6-null mice were housed singly with an 8-week old C57BL/6J mouse. The numbers of litters born and the number of pups per litter were recorded over a period of 90 days. For serum hormone analysis, mice were

euthanized by overdose of 5% avertin and blood was collected by cardiac puncture. Serum was separated by centrifugation and stored at -20^{o}C prior to radioimmunoassay (RIA) analysis at the Center for Research in Reproduction Ligand Assay and Analysis Core at the University of Virginia. All females were sacrificed when they were in the diestrus stage of the estrous cycle.

GnRH dose response and pituitary stimulation tests. To determine the appropriate dose of GnRH required to evoke a significant increase in serum LH levels, adult C57BL/6J male mice (n=3) were injected subcutaneously with varying concentrations (100, 200 or 400 ng/kg) of GnRH (Sigma-Aldrich) dissolved in 0.9% saline, or with vehicle. Exactly 10 min after the injection, blood was collected by cardiac puncture. Serum was separated by centrifugation and stored at -20^{o}C prior to analysis using the LUMINEX system at the Center for Research in Reproduction Ligand Assay and Analysis Core at the University of Virginia. From this preliminary experiment, we established that 200 ng/kg GnRH was an appropriate sub-maximal dose for determining the pituitary responsiveness of Six6KO males. From experimental wild-type (n=3) or homozygous Six6-null (n=3) mice, a small sample of blood (100 µl) was taken, via tail bleed, to serve as a baseline for LH levels. After three days recovery, mice were given an injection of either 200 ng/kg GnRH or vehicle (saline). Exactly 10 min after the injection, blood was collected by tail bleed and serum analyzed as stated above.

Gonadal histology. Ovaries and testes were dissected and weighed from animals for each of the three genotypes. Ovaries were fixed for 1-2 hours at room temperature (RT) in 4% paraformaldehyde (PFA, Fisher) in PBS. Testes were fixed for 8 hours in Bouin's fixative (Sigma) at RT. Gonads were paraffin embedded,

serially sectioned at 10 μm and stained with hematoxylin and eosin (H&E, Sigma). Histology was examined and the presence or absence of corpora lutea in the ovaries recorded.

LHβ Immunohistochemistry. Pituitaries were dissected out and fixed for 1-2 hours at RT in 4% PFA. After processing for paraffin embedding they were serially sectioned at 7 μm. The primary antibody used was rabbit anti-rat LHBeta (anti-rat Beta LH-IC-3; 1:1000 dilution in 5% goat serum/0.3% Triton X-100). Biotinylated goat-anti-rabbit IgG (Vector Laboratories, 1:300 dilution) was used as a secondary antibody and LHβ peptide was visualized using the Vectastain ABC elite kit and VIP peroxidase kit (Vector Labs). In order to quantify the LHBeta expression, a single section through the middle of each pituitary was visualized through the microscope and all positive cells within the section counted (n=4 for each genotype).

Hypothalamic GnRH content. Hypothalami were dissected from 4 month-old female mice in diestrus, snap frozen and stored at -80^{o}C until processed. RNA was extracted using Trizol (Invitrogen) according to manufacturer's instructions and reverse transcribed using First Strand cDNA Synthesis Kit (GE Healthcare) according to manufacturer's instructions. Q-RT-PCR was performed as previously described (Larder, 2009). See Table 1.1 for primer sequences.

Embryo collection. Embryos were generated through timed-breeding of adult heterozygotes with embryonic day (e) 0.5 being noon of the day the vaginal plug was detected. Plugged females were euthanized, and embryos were harvested at e13.5. A small amount of the tail was removed from each embryo and used to extract DNA for genotyping (See Table 1.1 for primers). Whole embryos were fixed in 10% acetic acid, 30% formaldehyde, 60% ethanol, overnight at 4°C and dehydrated in 70% EtOH

prior to embedding in paraffin. Sagittal sections (10 μm) were floated onto SuperFrost Plus slides (Fisher). Approximately 150 sections were processed and stained per embryo.

Embryonic GnRH Immunohistochemistry. Immunohistochemistry was performed as previously described (Miller, 2009). The primary antibody used was anti-GnRH antibody (Affinity BioReagents PA1-121; 1:1000 dilution in 5% goat serum/0.3% Triton X-100). Biotinylated goat-anti-rabbit IgG (Vector Laboratories, 1:300 dilution) was used as a secondary antibody and GnRH peptide was visualized using the Vectastain ABC elite kit and VIP peroxidase kit (Vector Labs). Sections were counterstained using methyl green (Vector Labs). GnRH neurons were counted in three or more embryos of each genotype analyzed. Cells were divided into nasal, cribriform plate, and brain regions and the mean calculated.

Adult brain Immunohistochemistry. Adult mice (4-5 months old) were anesthetized with 5% avertin then transcardially perfused with 20 ml PBS followed by 20 ml 4% PFA, pH 7.4. Adult females were sacrificed during diestrus. Postnatal day 1 (P1) mice were sacrificed at birth by decapitation. Brains were dissected out and incubated in 4% PFA overnight at 4^{o}C. Following embedding, each brain was serially sectioned in 12 μm coronal sections onto GOLD SuperFrost Plus slides (Fisher). Approximately 250 sections were processed per mouse. GnRH immunohistochemistry was performed as described above. Tyrosine hydroxylase immunohistochemistry was performed as described above using a rabbit polyclonal anti-tyrosine hydroxylase antibody (Pel-Freez Biologicals, P40101; 1:1000 dilution in 5% goat serum/0.3% Triton X-100). Secondary antibody and chemical visualization steps were performed as for GnRH immunohistochemistry.

Bioinformatic analysis. Approximately 2000 bp of GnRH upstream regulatory region sequence was obtained for rat, mouse, human, dog, horse, cow, shrew, and bat using Ensembl. Sequences were aligned using the ClustalW program (available from the European Bioinformatics Institute) and imported into GeneDoc (available from The National Resource for Biomedical Supercomputing) for annotation.

Expression plasmids. Mouse Six6 was amplified by RT-PCR from GT1-7 cell cDNA and the product was TOPO-cloned into pCR2.1 (Invitrogen). After sequence verification, Six6 was subcloned into pSG5 (Stratagene; pSG5-Six6) and p3xFLAG-CMV7.1 (Sigma-Aldrich; pCMV-Six6-FLAG). Mouse Six3 expression plasmid (pCMV-HA-Six3) was obtained from G. Olivier and subcloned into pSG5 (pSG5-Six3). Six3DelN expression plasmid (pSG5-Six3DelN) was generated by PCR from the wild-type plasmid and corresponds to amino acids 80-333 (primers in Table 1.1). The mouse Msx1 expression plasmid (pCB6+Msx1) was obtained from C. Abate-Shen, the mouse Dlx5 expression plasmid (pcDNA3-Dlx5) was obtained from J.L.R. Rubenstein and the mouse Otx2 expression plasmid (pSG5-Otx2) was obtained from A. Simeone.

Cell culture and transient transfections for luciferase reporter assays. All cells were cultured in DMEM (Mediatech) containing 10% fetal calf serum (Gemini Bio-Products), and 1% penicillin/streptomycin (Invitrogen) in a humidified 5% CO_2 incubator at 37^{o}C. Cells were seeded into 24-well plates and incubated overnight at 37^{o}C before being transiently transfected using FuGENE reagent (Roche Applied Science). Luciferase reporters were pGL3-GnRHe/p [rat GnRH enhancer (-1863 bp to -1571 bp) fused to the rat GnRH promoter (-173 bp to +112 bp)]; pGL3-5kb-GnRH (5 kb of the rat GnRH regulatory region); pGL3-ATTA-multimer [five copies of -48 bp

to -55 bp of the rat GnRH promoter fused to a herpes simplex virus thymidine kinase (TK) promoter]; pGL3-GnRHe/p-E+Pdel [GnRHe/p with all four ATTA sites deleted]; pGL3-GnRHe/p-EDel [GnRHe/p with both Enhancer ATTA sites deleted]; pGL3-GnRHe/p-Pdel [GnRHe/p with both promoter ATTA sites deleted]. Cells were transfected with 200 ng of expression plasmid, 400 ng of luciferase-reporter plasmid and 100 ng of the internal-control TK -109 bp promoter on β-galactosidase. For titration experiments (Fig. 6D), cells were co-transfected with 200 ng of Six3 expression plasmid and either 50 ng, 100 ng or 200 ng of Six6 expression plasmid along with 400 ng of pGL3-GnRHe/p luciferase-reporter plasmid and 100 ng of the internal control TK -109 bp promoter. Cells were harvested after 48 h, lysed then assayed for luciferase and β-galactosidase as previously described (Mcgillivray, 2005). Luciferase values were divided by β-galactosidase values to control for transfection efficiency. All experiments were performed in triplicate and repeated a minimum of three times.

Electrophoretic mobility shift assays (EMSA). EMSA oligonucleotides (Table 1.1) were annealed, end-labeled, then purified as previously described (Cherrington, 2008). Binding reactions used 2 fmol of [^{32}P]-labeled oligonucleotide and either 2 µg of GT1-7 nuclear protein, 1 µg Cos-cell nuclear protein transfected with pCMV-3XFLAG, or 1 µg of nuclear protein from Cos-cells transfected with p3XFLAG-CMV7.1. After addition of the probe, binding reactions were incubated for 10 min at RT prior to electrophoresis on a 5% polyacrylamide gel in 0.25x TBE (Tris-Borate-EDTA). Competition assays were performed by pre-incubating the reactions with 500-fold excess of unlabeled oligonucleotide for 5 min prior to addition of probe. For supershift assays, 2.5 µg of an ANTI-FLAG M2 Monoclonal antibody

(Sigma-Aldrich), or normal mouse IgG control (Santa Cruz Biotechnology), was added to the reaction. Gels were electrophoresed at 250 V for 2 h then dried, under vacuum, and exposed to film.

Statistical Analysis. Raw data were analyzed by one-way ANOVA, followed by post-hoc comparisons with the Tukey-Kramer honestly significant difference test using statistical package JMP 8.0 (SAS). Significant differences were designated as $p < 0.05$.

Chapter 1.3: Results

Six6 expression is dramatically induced in a mature GnRH neuronal cell line

To identify candidate genes critical for the maturation of the GnRH neuronal phenotype, we performed an Affymetrix microarray screen comparing RNA from GN11 cells (representing an early stage of development) and GT1-7 cells (representing a more mature hypothalamic neuron). Analysis of the results determined that more than 2000 transcripts showed significantly higher levels of expression in the more mature, GT1-7 cells versus the immature GN11 cells (data not shown). Unsurprisingly, several of these differentially regulated transcripts have previously been reported as being important for regulation of GnRH transcription such as Otx2 (Kelley, 2000; Larder, 2009), Dlx5 (Givens, 2005), Gata4 (Lawson, 1998), Msx1 (Givens, 2005), and Pbx1 (Rave-Harel, 2004). Intriguingly, we observed that Six6, a homeodomain-containing protein, known to be expressed in the pituitary and hypothalamus (Jean, 1999), was one of the most differentially regulated transcripts on the microarray (~208-fold higher expression in GT1-7 cells compared to GN11 cells). Semi-quantitative RT-PCR validated the differential expression of Six6 mRNA

between the two cell lines (Fig. 1.1*A*), and confirmed previous reports demonstrating that Six6 is expressed within adult mouse pituitary, hypothalamus and eye (Conte, 2005; Li, 2002). In addition, quantitative RT-PCR confirmed the differential expression profile of Six6 and Six3 in the two model cell lines (Fig. 1.1*B*), with Six6 up-regulated to a similar degree to that seen in the microarray (~180 fold). Although Six3 is in the same subfamily as Six6 (Kumar, 2009), it is not differentially expressed between the two cell lines, and, as previously shown (Conte, 2005), is not detected in the adult hypothalamus (Fig. 1.1*A* and 1.1*B*). Given that the observed increase in Six6 expression correlated with an increase in GnRH expression, we hypothesized that Six6 may regulate GnRH gene expression and thus play an important role in hypothalamic control of fertility.

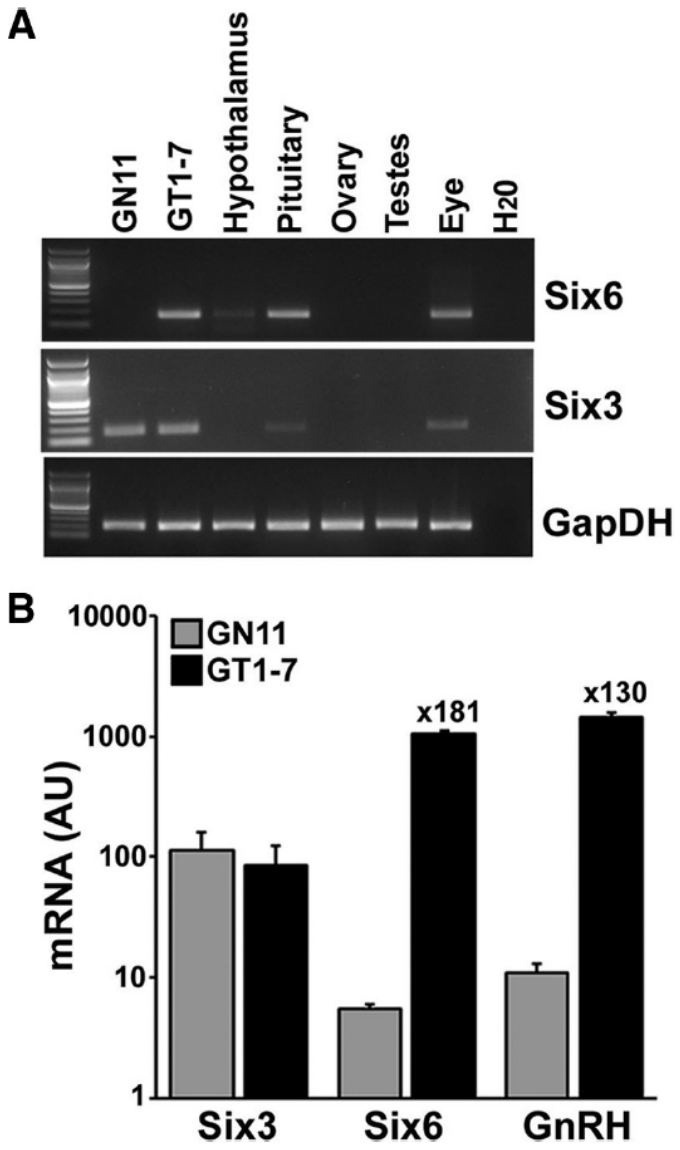

Figure 1.1. Six6 expression is dramatically increased in the mature GnRH neuronal GT1-7 cell line. ***A****,* RT-PCR analysis of Six6 and Six3 expression in various adult mouse tissues and two GnRH neuronal cell lines. GapDH was used as a positive control. ***B***, Quantitative RT-PCR analysis of Six6, Six3, and GnRH mRNA extracted from GN11 and GT1-7 cells. Results are expressed as arbitrary units (AU) of GnRH mRNA levels normalized against GapDH mRNA levels and are the mean of three separate experiments performed in triplicate. Results shown are average ± SEM. Numbers above the GT1-7 bar indicate fold increase in mRNA levels in GT1-7 cells compared to GN11 cells.

Loss of Six6 expression disrupts male fertility due to decreased FSH release

Initial reports characterizing the Six6-null mouse focused on its role during eye development. While the knock-out mice were reported to have hypoplastic pituitary glands, the presence of all the pituitary hormones was confirmed and the fertility of the mice was not reported (Li, 2002). To determine whether loss of Six6 expression results in compromised fertility, we performed a fertility assessment of wild-type, heterozygous and homozygous Six6-null littermates. At 8 weeks of age, each male mouse was paired with an 8-week old C57BL/6J female and the frequency and size of any litters born recorded for 3 months. While homozygous (KO) males were fertile, they produced significantly reduced numbers of litters during the 3-month assessment period when compared to their wild-type (WT) and heterozygous (HET) littermates (Table 1.2). The number of pups per litter was not significantly different between the three genotypes, suggesting comparable embryonic viability (Table 1.2).

Table 1.2. Male fertility assessment. Results shown are average ± SEM. ANOVA with *post hoc* Tukey test were performed on WT vs. HET; WT vs. KO and HET vs. KO and established statistical significance '*' as $p<0.05$.

	# Litters in 3 months	# Days till 1st Litter	# Pups per litter
WT	2.8 ± 0.2 (n=6)	23 ± 1.0 (n=6)	8.3 ± 0.8 (n=16)
HET	2.8 ± 0.4 (n=5)	25 ± 1.6 (n=5)	8.8 ± 0.6 (n=14)
KO	1.8 ± 0.3* (n=6)	34 ± 5.6 (n=6)	6.9 ± 0.8 (n=12)

Changes in gonadotropin hormone release in these mice were measured by radioimmunoassay (RIA). While all serum gonadotropins (FSH, LH and testosterone [T]) were reduced in the KO males, compared to their WT littermates, only the decrease in FSH levels reached statistical significance (Figs. 1.2*A*, 1.2*B* and 1.2*C*). With KO mice showing both decreased fertility and serum gonadotropins, we sought to determine whether Six6-null males had any obvious gonadal abnormalities. Comparison of sperm counts (Fig. 1.2*D*) and testes weights (Fig. 1.2*E*) revealed no significant differences between the three genotypes; however, seminal vesicle (SV) weight was significantly reduced in the KO males (Fig. 1.2*E*). This result is consistent with the decreased testosterone levels seen in these animals (Fig. 1.2*C*) since SV tissue is responsive to T (Shima, 1990). Given that histological examination of WT, HET and KO testes revealed no striking differences in either architecture or spermatogenesis (Fig. 1.2*G-I*), we analyzed other reproductive functions in these mice. We hypothesized that the lowered SV weight in these mice might lead to a decrease in seminal fluid volume (Bradshaw, 1977). Analysis of the ability of WT, HET and KO males to produce vaginal plugs in wild-type females confirmed this hypothesis: only 33% of females housed with a KO male formed a visible plug after 10 days of cohabitation compared to 100% of females housed with either a WT or HET male (Fig. 1.2*F*).

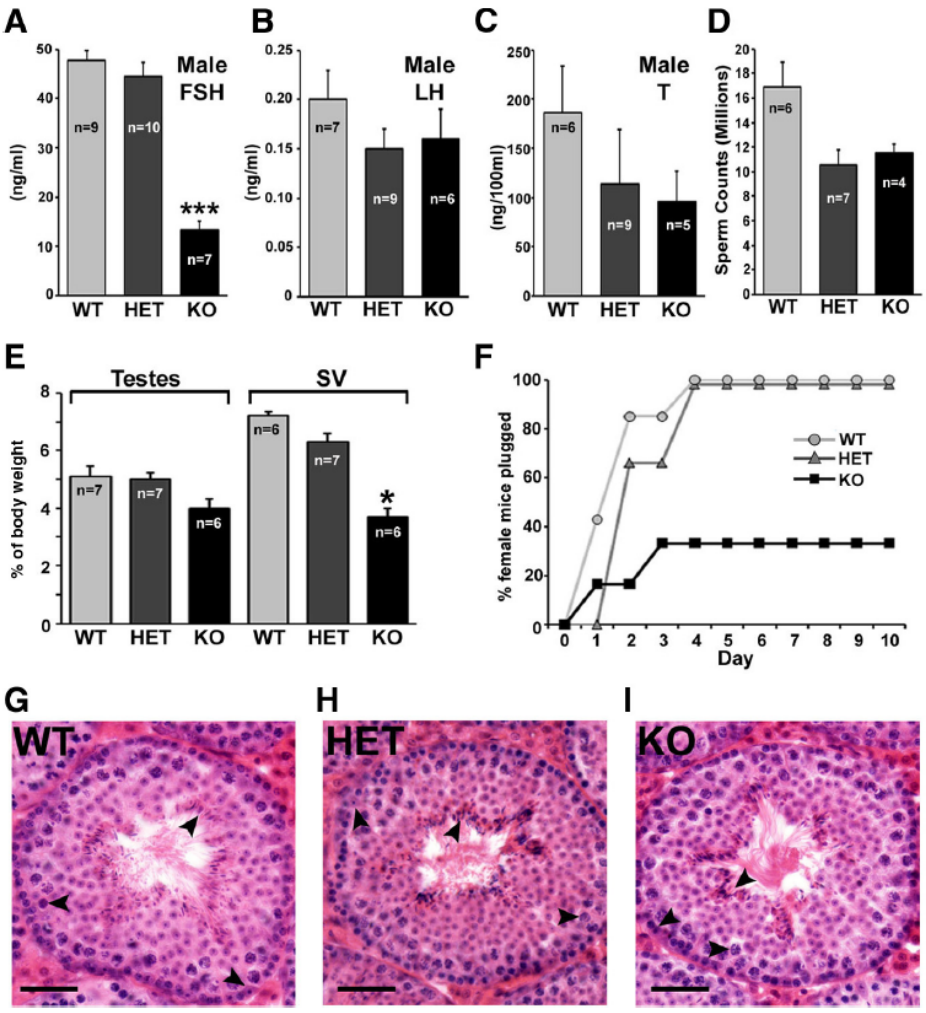

Figure 1.2. Reproductive phenotype of Six6-null male mice. ***A,*** Average serum FSH levels of 4-6 month old WT, HET and KO male mice. ***B,*** Average serum LH levels of 4-6 month old WT, HET and KO male mice. ***C,*** Average serum testosterone (T) levels of 4-6 month old WT, HET and KO male mice. ***D,*** Average sperm count of 4-6 month old WT, HET and KO male mice. ***E,*** Average relative testis and seminal vesicle (SV) weight of 4-6 month old WT, HET and KO mice. ***F,*** Percentage of wild-type females that plug after 10 consecutive days of mating with either a WT, HET or KO male mouse. ***G, H and I,*** H&E stained testes sections from wildtype (WT, panel G), heterozygous (HET, panel H) and homozygous (KO, panel I) Six6-null mice. Sertoli cells, primary spermatagonia and elongated spermatids are indicated with arrowheads in each section. No abnormal histology was observed between the three genotypes examined. Magnification is 40x and scale bars represent 10 μm. Results shown are average ± SEM. ANOVA with *post hoc* Tukey test were performed on WT vs. HET; WT vs. KO and HET vs. KO and established statistical significance '*' as $p<0.05$ and '***' as $p<0.001$.

Loss of Six6 expression severely disrupts female fertility

The fertility of female Six6-null mice was also assessed over a 3-month period. As expected, wild-type and heterozygous females demonstrated normal reproductive behavior (Table 1.3). In contrast, the fertility of KO females was severely compromised with only one of the eight females assessed (12.5%) producing a single litter of five pups, 27 days after being paired with a male (Table 1.3).

Table 1.3. Female fertility assessment. Results shown are average ± SEM. ANOVA with *post hoc* Tukey test were performed on WT vs. HET; WT vs. KO and HET vs. KO and established statistical significance '***' as $p<0.001$.

	# Litters in 3 months	# Days till 1st Litter	# Pups per litter	Day of Vaginal Opening
WT	2.6 ± 0.3 (n=7)	24 ± 1.9 (n=7)	8.3 ± 0.7 (n=18)	27 ± 0.3 (n=12)
HET	2.1 ± 0.5 (n=7)	26 ± 2.7 (n=6)	7.1 ± 0.8 (n=16)	27 ± 0.5 (n=12)
KO	0.13 ± 0.1 *** (n=8)	27 (n=1)	5 (n=1)	28 ± 0.2 (n=5)

Six6-null females display normal puberty but have disrupted estrous cycles

In female rodents, normal initiation of puberty results in vaginal opening followed by the beginning of regular estrous cycles. To assess puberty in Six6-null mice, female pups were observed daily for vaginal opening beginning at time of weaning (20 d). No significant differences in day of vaginal opening were observed between the three genotypes examined (Table 1.3), suggesting that loss of Six6 expression does not alter onset of puberty. To assess estrous cyclicity, vaginal

cytology of wild-type (WT), heterozygous (HET) and homozygous (KO) Six6-null littermates was examined daily by vaginal lavage. Mean cycle length was doubled in KO mice compared to their WT and HET littermates resulting in the KO females spending significantly more of the cycle in estrus (Fig. 1.3*A*-*C*).

Ovarian histology is abnormal in Six6-null females

To examine folliculogenesis and ovulation in Six6-null mice, diestrus ovaries from 4-6 month old mice were inspected for developing follicles and corpora lutea (CL). Ovaries from KO mice were significantly smaller (Fig. 1.3*G*) and had significantly fewer CL (Fig. 1.3*H*) than ovaries from WT or HET littermates. Histological analysis revealed that ovaries from WT and HET mice displayed normal folliculogenesis (Figs. 1.3*D, E and H*). In contrast, of the five ovaries analyzed from KO mice, CL were only detected in the ovaries of the single Six6-null mouse that produced one litter during the fertility assessment (Fig. 1.3*H*). Furthermore, closer examination of all the KO ovaries revealed the presence of abnormal stromal tissue consisting of cells with enlarged cytoplasm, indicative of a failed attempt to transform granulosa cells into luteal tissue (Fig. 1.3*I* and 1.3*J*). In addition, large cystic follicles (CF, Fig. 1.3*F*) were also commonly observed in the ovaries of Six6-null animals.

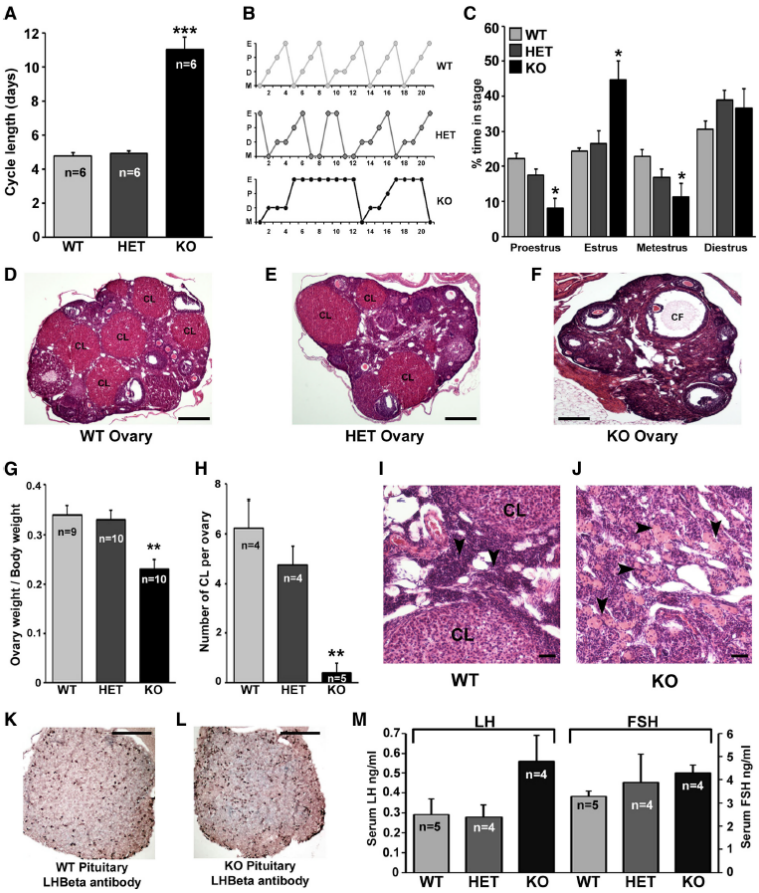

Figure 1.3. Reproductive phenotype of Six6-null female mice. ***A,*** Average estrous cycle length of WT, HET and KO females. ***B,*** Representative estrous cycles as measured by vaginal cytology. E, estrus; P, proestrus; D, diestrus; M, metestrus. ***C,*** Percentage of time during a single estrus cycle that is spent in each stage. ***D, E and F,*** H&E-stained ovarian sections from wildtype (WT, panel D), heterozygous (HET, panel E) and homozygous (KO, panel F) Six6-null mice. KO ovaries exhibit large cystic follicles (CF) and no corpora lutea (CL). Magnification is 4x and scale bars represent 100 µm. ***G,*** Average relative ovary weight of 4-6 month old WT, HET and KO mice. ***H,*** Average number of corpora lutea (CL) in ovaries of WT, HET and KO Six6-null females. ***I*** and ***J,*** H&E stained ovaries from wild-type (WT) and homozygous Six6-null mice (KO) showing stromal tissue. Extensive areas of cells with enlarged cytoplasm (arrowheads) are seen in the stroma of KO mice. Magnification is 20x and scale bars represent 10 µm. ***K and L,*** Luteinizing Hormone Beta subunit (LHBeta) staining of the anterior pituitaries of 6 month old WT and KO female mice. Magnification is 10x and scale bars represent 10 µm. ***M,*** Serum LH and FSH levels of 4-6 month old, diestrus stage, WT, HET and KO female mice. KO mice had increased levels of LH compared to WT and HET littermates (p=0.056). There was no difference in FSH levels between the three genotypes. Results shown are average ± SEM. ANOVA with *post hoc* Tukey test were performed on WT vs. HET; WT vs. KO and HET vs. KO and established statistical significance '*' as $p<0.05$; '**' as $p<0.01$; '***' as $p<0.001$.

Basal serum gonadotropin levels are not significantly altered in Six6-null females

Because Six6 has been reported to be expressed in both the developing and mature pituitary (Jean, 1999; Li, 2002) and Six6-null females appear to have defective ovulation (Fig. 1.3*F*), we wished to determine whether Six6-null mice have normal expression of luteinizing hormone beta (LHβ) from gonadotrope cells within the anterior pituitary. Immunohistochemistry revealed no significant difference in either gonadotrope cell number or expression of LHβ when pituitaries from wild-type mice were compared to those from homozygous Six6-null littermates (Figs. 1.3*K* and 1.3*L*; WT: 252 positive cells ± 27 vs. KO: 297 positive cells ± 48; p=0.44 t-test). This suggests that loss of Six6 expression does not affect the ability of the gonadotrope to produce LHβ. RIA measurement of serum gonadotropins revealed that while neither LH or FSH concentrations were significantly different between the three genotypes, serum LH levels were almost doubled in KO females, though this did not reach statistical significance (Fig. 1.3*M*), increased serum LH is consistent with the cystic follicles seen in these animals (Fig. 1.3*F*).

Six6-null mice have significantly decreased hypothalamic GnRH expression

Since Six6-null ovaries showed no evidence of ovulation, and females had increased expression of pituitary LHβ, it was important to determine the levels of GnRH expression in the hypothalami of these mice. Analysis of protein expression using a GnRH antibody revealed that Six6KO mice had dramatically reduced numbers of GnRH neurons (Figs. 1.5*A* and 1.5*B*). Cell counts from coronal sections extending from the medial septum through to the anterior hypothalamus revealed an

89% decrease in total GnRH neuron numbers in 4-month old KO females when compared to their WT littermates (Table 1.4). A similar decrease was seen in 4-5 month old Six6KO male mice (Table 1.4).

Table 1.4. GnRH neuron counts. Results shown are average ± SEM. ANOVA with *post hoc* Tukey test were performed on WT vs. HET; WT vs. KO and HET vs. KO and established statistical significance '***' as $p<0.001$.

	Female adult	**Male adult**	**Post-natal Day 1**	**Embryonic Day 13.5**
WT	442 ± 27 (n=3)	488 ± 51 (n=3)	254 (n=1)	449 ± 41 (n=3)
KO	47 ± 12 *** (n=3)	77 ± 15 *** (n=3)	96 ± 30 (n=3)	425 ± 28 (n=3)

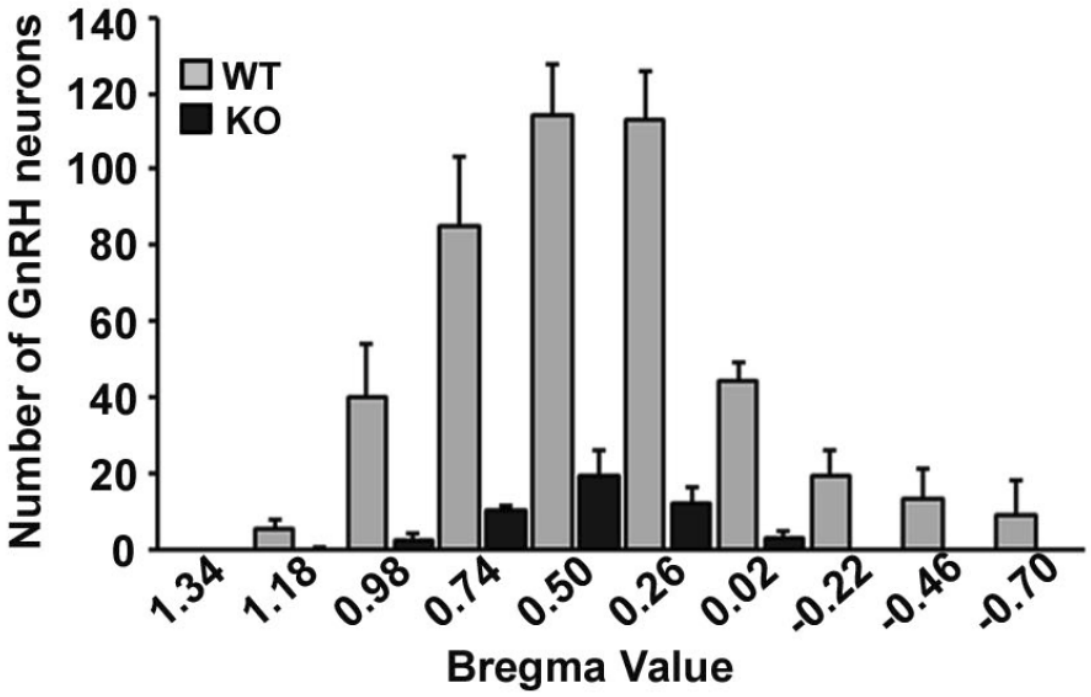

Figure 1.4. Average GnRH neuron counts in relation to their position within the brain. Positions are given relative to Bregma values. One bar corresponds to 240 μm. Bregma point 0.5 corresponds to the OVLT.

The location of the GnRH neurons was mapped within the brain, revealing that the significant decrease in neuron numbers affected all the brain regions analyzed (Fig. 1.4). Immunostaining of the median eminence (ME) showed a similar marked decrease in GnRH neuron axon density (Figs. 1.5*C* and 1.5*D*). The decrease in GnRH protein expression was then confirmed at the mRNA level by Q-RT-PCR analysis of hypothalami from adult WT and KO mice. Loss of Six6 resulted in an ~83% decrease in GnRH mRNA expression (Fig. 1.5*I*). To determine whether other neuronal cell types are also affected by the loss of Six6, expression of tyrosine hydroxylase (TH) throughout the brain of WT and Six6KO animals was also analyzed.

TH is the first enzyme in the catecholamine (CA) biosynthesis pathway catalyzing the conversion of L-tyrosine to L-DOPA and is, therefore, a useful marker of all CA-positive neurons. Our analysis revealed that female Six6-null mice have decreased numbers of TH-positive neurons within the anteroventral periventricular (AVPV) region (Figs. 1.5*E* and 1.5*F*) and also show decreased targeting to the ME (Figs. 1.5*G* and 1.5*H*). The rodent AVPV is sexually dimorphic, with females showing a greater number of TH-positive neurons than males (Simerly, 1985). Whether the observed decrease in TH-positive AVPV neurons in female Six6KO mice represents a deficit in the sexual dimorphism of the brain, or represents a more general hypothalamic defect, awaits further investigation; however, our analysis of vaginal opening (Table 1.3) suggests the latter and indicates that the hypothalamic effects of deleting Six6 may not be confined to the GnRH neuronal population.

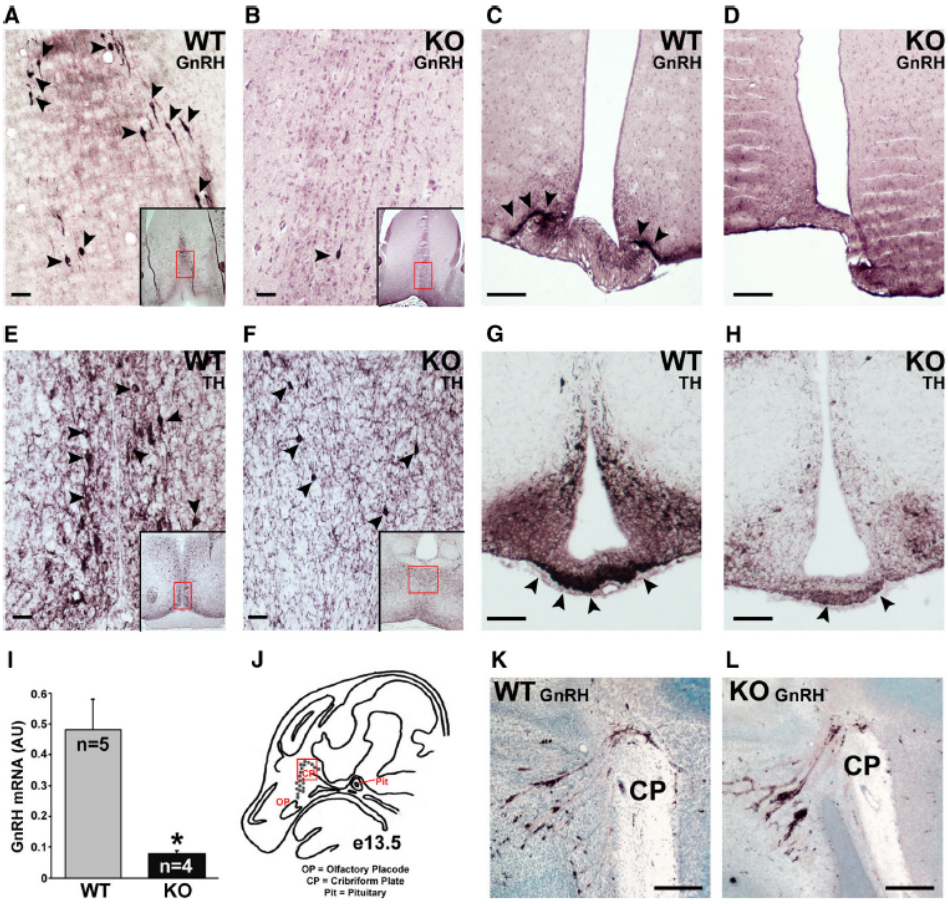

Figure 1.5. Adult Six6-null mice have a significant reduction in GnRH neuron numbers. A-D, Coronal brain sections showing GnRH staining in the hypothalamus (panels A and B) and median eminence (panels C and D). The red box in panels A and B indicates the area of the section that has been enlarged. Black arrowheads indicate GnRH neurons in panels A and B and GnRH axons in panel C. ***E, F, G and H,*** Coronal brain sections showing tyrosine hydroxylase (TH) staining in the anteroventral periventricular (AVPV) nucleus (panels E and F) and median eminence (panels G and H). The red box in panels E and F indicates the area of the section that has been enlarged. Black arrowheads indicate TH neurons in panels E and F and TH axons in panel G. Scale bars represent 10 μm in panels A, B, E and F and 100 μm in panels C, D, G and H. ***I,*** Quantitative RT-PCR analysis of hypothalamic GnRH mRNA in 4-6 month old WT and KO female mice. Results are expressed as arbitrary units (AU) of GnRH mRNA levels normalized against GapDH mRNA levels and are the mean of three separate experiments performed in triplicate. ANOVA with *post hoc* Tukey test established statistical significance '*' as $p<0.05$. ***J,*** Diagram of e13.5 mouse head anatomy in a sagittal section showing the location of migrating GnRH neurons. Red box indicates the field shown in panels K and L. ***K and L***, Immunohistochemical staining for GnRH in e13.5 wild-type (WT, panel K) and Six6-null (KO, panel L) embryos. Magnification is 10x and scale bars represent 50 μm. CP; cribriform plate.

The decrease in GnRH neuron numbers in Six6KO mice occurs during late embryonic development

GnRH neurons are first observed within the olfactory placode at around embryonic day (e) 10.5. From there they migrate across the cribriform plate and through the basal forebrain to arrive at the presumptive hypothalamus at around e17.5. To establish whether the loss of GnRH neurons observed in Six6-null adults occurs during embryonic development, the total number and distribution of GnRH-positive neurons was evaluated in e13.5 and post-natal day 1 (P1) animals. WT and KO embryos were sagittally sectioned, stained for GnRH protein, and positive neurons counted. In contrast to the results observed in adult mice, total numbers of GnRH neurons at e13.5 were not significantly different between WT and KO littermates (Table 1.5). Furthermore, there was no disruption to the progress of the GnRH neurons along their migratory path (Figs. 1.5*K*, 1.5*L* and 1.6). However, similar to our observations in adult mice, a substantial decrease in GnRH neuron numbers was seen in Six6 null animals at P1 (Table 1.5) leading us to hypothesize that a similar decrease in GnRH mRNA would also been seen at this time-point. Taken together these data suggest that Six6 is not required for either the birth or initial migration of GnRH neurons, nor is it essential for initiation of GnRH expression. However, as observed in the case of activator protein-2 (AP-2) expression (Kramer, 2000), as the GnRH neuron matures during adulthood, and GnRH expression increases, expression of Six6 is required to ensure that normal adult levels of GnRH transcription are achieved and maintained.

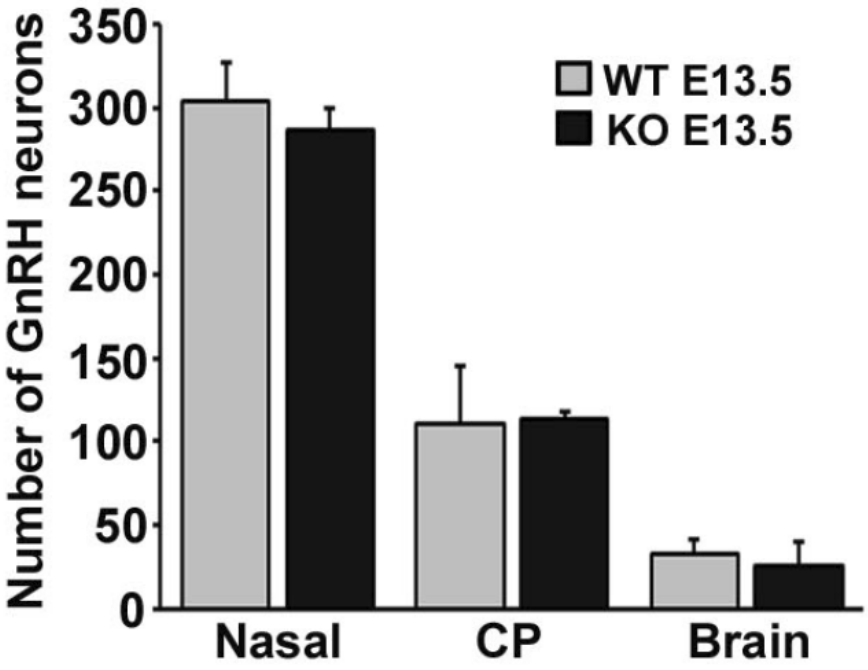

Figure 1.6. Average numbers of GnRH neurons counted in the nasal, cribriform plate (CP) or brain regions of WT and KO mice at embryonic day (e) 13.5.

Six6KO null males are able to generate a normal LH surge in response to GnRH

Given that Six6 is expressed in the pituitary (Fig. 1.1*A*), it is possible that the fertility effects observed in these animals may be due, in part, to the loss of Six6 expression within gonadotrope cells. Therefore, it was important to establish whether the pituitaries of these animals were functioning normally with respect to gonadotropin release in response to GnRH. Male mice were injected with a bolus of GnRH and blood collected 10 minutes later for analysis of serum gonadotropins levels. All analysis was performed on male mice to rule out any complications due to the stage of the estrus cycle and steroid feedback from the ovaries. Analysis revealed that all doses of GnRH used (100, 200 or 400 ng/kg) resulted in a significant increase in LH serum levels (Fig. 1.7*A*). Furthermore, a small, but not significant, increase in FSH serum levels was also observed at all concentrations tested (Fig. 1.7*C*). Given this, we chose 200 ng/kg GnRH as an appropriate dose to determine whether a significant increase in serum LH would also be observed in Six6 null animals. While no difference in basal LH serum levels was detected between the two genotypes (due to the sensitivity of the assay being 0.48 ng/ml) both WT and KO males showed a dramatic increase in LH serum levels 10 minutes after injection with 200 ng/kg GnRH (Fig. 1.7*B*) suggesting that the pituitaries of Six6KO mice can respond appropriately when presented with GnRH. Finally, while a difference in baseline FSH levels was observed between the two genotypes, confirming data shown in Figure 2, both WT and KO mice showed a small increase in FSH secretion in response to GnRH (Fig. 1.7*D*).

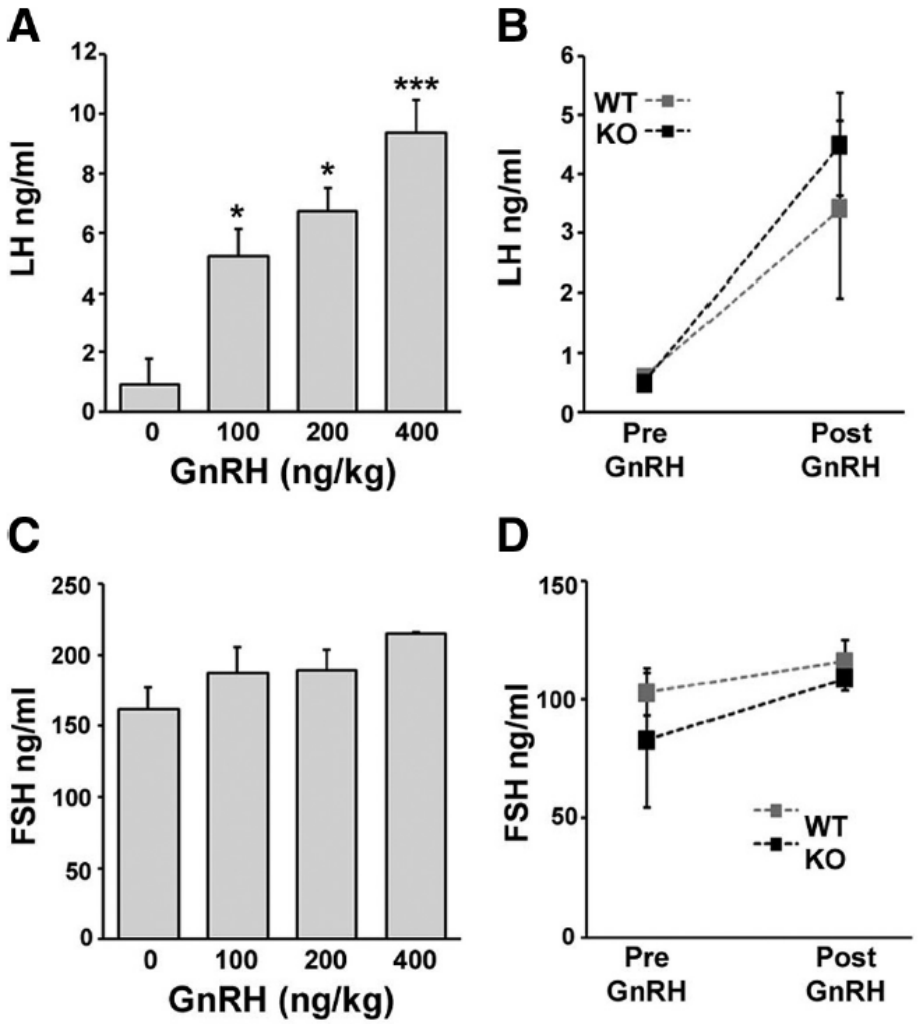

Figure 1.7. Six6KO male mice respond normally to a surge of GnRH. ***A****,* Effect of increasing doses of GnRH on WT LH serum levels. ***B***, LH serum levels of WT and KO male sib pairs prior to, and 10 minutes after, injection of 200 ng/kg GnRH. ***C****,* Effect of increasing doses of GnRH on FSH serum levels. ***D***, FSH serum levels of WT and KO male sib pairs prior to, and 10 minutes after, injection of 200 ng/kg GnRH. Results shown are average ± SEM. ANOVA with *post hoc* Tukey test comparing each GnRH treatment to the control (saline) established statistical significance '*' as $p<0.05$ and '***' as $p<0.001$.

Overexpression of Six6 increases GnRH transcriptional activity in both GnRH neuronal cell lines

Given that Six6-null adults have such a dramatic decrease in both GnRH mRNA and protein expression, we next investigated the role of Six6 in transcriptional control of GnRH gene expression. Six6 was overexpressed by transient transfection in GN11 and GT1-7 cells along with either -5 kb of the rat GnRH regulatory region or the previously characterized rat GnRH enhancer and promoter (GnRHe/p), fused upstream of a luciferase reporter gene (Lawson, 2002) (Fig. 1.8*A*). Overexpression of Six6 significantly increased the activity of both of the luciferase reporter genes tested, in both cell lines (Fig. 1.8*B*). When the same experiments were performed using a Six3 expression plasmid, contrasting results were observed. Six3 significantly activated both luciferase reporters in GN11 cells; however, in the GT1-7 cells, overexpression of Six3 resulted in significant repression of GnRH promoter activity (Fig. 1.8*C*). Further experiments revealed that the repressive effects of Six3 on GnRH transcription in GT1-7 cells could be relieved by titrating in increasing amounts of Six6 (Fig. 1.8*D*), indicating a potential competition between the two factors for binding sites in the GnRH regulatory region.

N-terminus truncation of Six3 results in activation of the GnRH promoter

The homeodomain and Six domain are highly homologous between Six3 and Six6 proteins [Fig. 1.8*E*, homeodomain (HD) 77% identical, Six domain (SD) 99% identical]. The main divergence between the two proteins is seen in the C-terminus region common to both proteins (43% identical) and by the presence of an 80-amino acid, glycine-rich region, at the N-terminus of the Six3 protein. To determine whether

this additional N-terminus region was mediating the repressive effects of Six3 on the GnRH promoter in GT1-7 cells, we generated a mutant Six3 protein (Six3DelN) with a deletion of this 240 bp sequence (Fig. 1.8*E*). In contrast to the results observed with wild-type Six3, overexpression of Six3DelN in GT1-7 cells resulted in similar induction in GnRH promoter activity to that seen in response to Six6 (Fig. 1.8*B*). This suggests that the unique N-terminus region of Six3 is required for the repressive activity of Six3 in GT1-7 cells.

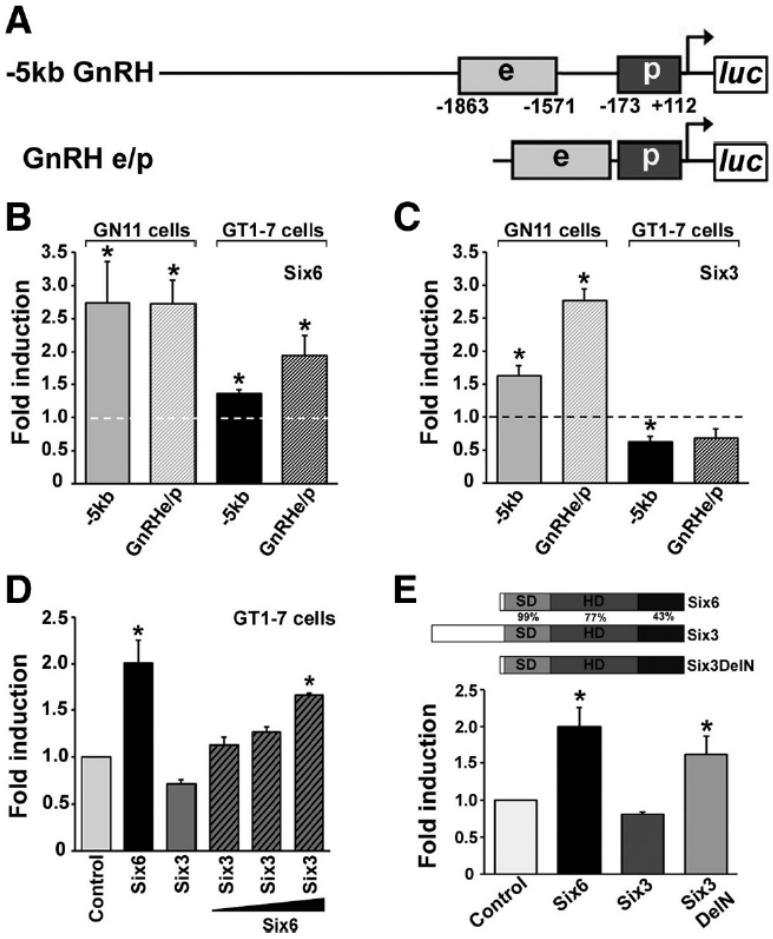

Figure 1.8. Six6 induces GnRH promoter activity. ***A****,* Schematic diagram showing the luciferase reporter constructs used in transient transfection assays. Numbers indicate the position of nucleotides relative to the transcription start site: promoter (p), enhancer (e), luciferase (luc). ***B*** *and* ***C***, Effect of over-expression of Six6 (B) or Six3 (C) on the -5 kb GnRH and GnRHe/p luciferase reporters in GN11 and GT1-7 cells. Fold-induction compared to 'empty' vector alone (dashed line) is indicated, corrected for β-galactosidase, which was used as an internal control. Over-expression of Six6 resulted in significant fold induction of both reporter constructs. Activation of promoter activity by Six3 was only seen in GN11 cells. ***D****,* Co-transfection of 200 ng Six3 expression plasmid and increasing amounts (50 ng to 200 ng) of Six6 expression plasmid relieves the repression of GnRHe/p promoter activity seen with Six3 alone. ***E****,* Over-expression of a mutant Six3 expression plasmid (Six3DelN) resulted in significant activation of GnRHe/p promoter activity in GT1-7 cells. SD, Six domain; HD, homeodomain. All experiments were performed in triplicate and repeated three times. Results shown are average ± SEM. One-way ANOVA with *post hoc* Tukey test established statistical significance as $p<0.05$. '*' represents significant activation vs. empty vector 'control'.

Six6 binds to conserved ATTA sites within the rat GnRH enhancer and promoter

In recent years, the regulatory target sequences of several Six proteins have been reported. Six1, Six2, Six4, and Six5 have been shown to bind to a TCAGGT sequence motif (Kawakami, 2000; Spitz, 1998). In contrast, Six3 and Six6 have been shown to bind to the classical homeodomain core sequence ATTA (Hu, 2008; Zhu, 2002), indicating that the DNA-binding specificity of the Six3/6 class of Six proteins differs from other members of the gene family. We have previously characterized a 173 bp promoter element and a 300 bp enhancer element within the rat GnRH regulatory sequence, both of which are essential for correct neuronal expression of GnRH (Lawson, 2002). Within these regions, several important transcription factor-binding sites have been identified including four ATTA sites that have previously been shown to be essential for cell-specific expression of the GnRH promoter (Kelley, 2002; Nelson, 2000). Bioinformatic analysis revealed a high level of conservation in the ATTA sites found in these regions between rat, mouse and human (Givens, 2004). To determine whether these ATTA binding sites are conserved across other species, the DNA sequences from -65 bp to -22 bp and from -1642 bp to -1603 bp of the rat GnRH regulatory sequence were aligned with the GnRH regulatory sequences from various mammals (Fig. 1.9*A*). The alignments show that all four ATTA motifs are well conserved, suggesting that all four sites are important for proper regulation of GnRH transcription. To analyze the affinity of Six6 for these ATTA binding sites, we performed Electrophoretic Mobility Shift Assays (EMSA) with radioactively labeled probes containing the -41 bp, -53 bp, -1622 bp, or -1635 bp sites (see Table 1.1). Nuclear protein extracts from COS-1 cells transiently transfected with FLAG-tagged

Six6 formed a specific complex when incubated with any of the four probes (Fig. 1.9*B*; lanes 2, 9, 16, and 23). This complex was not observed when nuclear extracts from COS-1 cells transfected with empty FLAG vector were incubated with the probes (lanes 1, 8, 15 and 22). This specific complex could be removed (lanes 10, 17 and 24) or supershifted (SS, lane 3) when incubated with an antibody to FLAG. Furthermore, the addition of unlabeled WT probe significantly decreased complex formation (lanes 6, 13, 20 and 27), whereas competition with an unlabeled, mutated probe (MUT, ATTA sequence mutated to GCCG) had no effect on complex formation (lanes 7, 14, 21 and 28). To show binding of endogenous Six6, EMSAs were also performed using nuclear extracts from GT1-7 cells and the -41 bp probe. This probe was selected because it shows 100% conservation of the ATTA sequence across various species analyzed (Fig. 1.9*A*). A specific complex formed on the – 41 bp probe (Fig. 1.9*C*, grey arrow, lane 2) and was competed away by addition of excess WT probe (lane 3), but not excess mutant probe (MUT, lane 4). As expected, this complex migrated slightly further on the gel than the complex formed by a FLAG-tagged Six6 protein overexpressed in Cos cells (black arrow, lane 1). Several other higher molecular weight complexes can also be seen (Fig. 1.9*C*, a-g) and likely correspond to other homeodomain containing factors, such as Msx and Dlx (Givens, 2005).

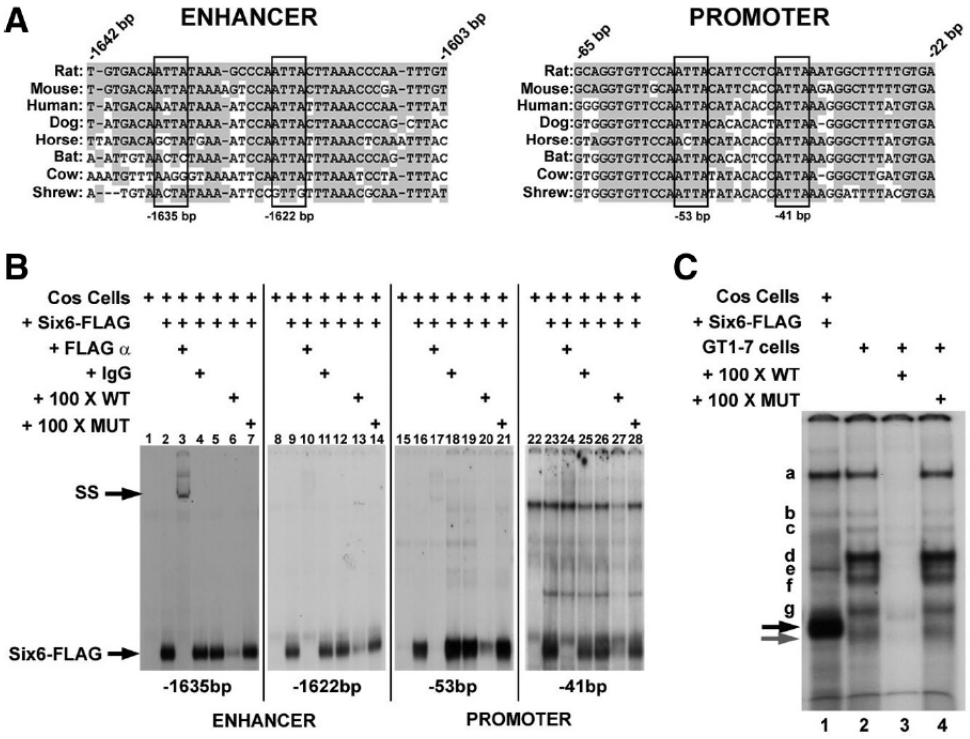

Figure 1.9. Six6 binds to ATTA sites within the rat GnRH promoter. ***A****,* The rat GnRH promoter sequence between -22 bp and -65 bp and enhancer sequence between -1603 bp and -1642 bp were aligned with sequences from the mouse, human, dog, horse, bat, cow, and shrew GnRH regulatory regions using the ClustalW program. Previously identified ATTA binding sites are enclosed in boxes. Nucleotides that are conserved between all the species are shaded grey. ***B****,* EMSA was performed with nuclear extracts from Cos cells transfected with either pCMV-FLAG (lanes 1, 8, 15 and 22) or pCMV-Six6-FLAG (all other lanes). The DNA probes consisted of radiolabeled oligonucleotides containing the ATTA sites identified at -41 bp, -53 bp, -1622 bp and -1635 bp of the rat GnRH regulatory region. A 500-fold excess of unlabeled wildtype (WT) or mutant (MUT) probe and an antibody against the FLAG tag (FLAG α) were included in the reaction mixtures as indicated. FLAG antibody was able to shift (SS) or remove a complex that formed on all probes after incubation with extracts from Cos cells transfected with pCMV-Six6-Flag. ***C****,* EMSA was performed with nuclear extracts from Cos cells transfected with pCMV-Six6-FLAG (lane 1) or GT1-7 cells (all other lanes). The DNA probe consisted of radiolabeled oligonucleotide containing the ATTA site identified at -41 bp of the rat GnRH regulatory region. A 500-fold excess of unlabeled wildtype (WT) or mutant (MUT) probe were included in the reaction mixtures as indicated. A complex corresponding to FLAG-tagged Six6 was observed in lane 1 (black arrow). A complex corresponding to endogenous Six6 protein was observed in lanes 2 and 4 (grey arrow). Various other complexes were also observed (a-g) and likely correspond to other homeodomain containing proteins.

Six6 regulates expression of GnRH via ATTA sites in the promoter

To verify the functional interaction of Six6 and the ATTA sites in the regulation of GnRH transcription, we performed transient transfection assays in both GnRH neuronal cell lines using a reporter plasmid containing five copies of the sequence from -44 bp to -35 bp of the rat GnRH regulatory region (ctcATTAaat). In this context, Six6 significantly activated the ATTA multimer by ~3-fold in both cell lines (Fig. 1.10*A*). To determine whether induction of the GnRH promoter by Six6 was dependent on the presence of intact ATTA sites, we deleted all four sites from the GnRHe/p luciferase reporter and analyzed the effects of Six6 on this mutated reporter (Fig. 1.10*B*). As previously reported (Givens, 2005), deletion of these four sites significantly reduced the luciferase activity of the mutant reporter (E+P Del) compared to wild-type (Fig. 1.10*B*), indicating that these sites are important for basal activity of the GnRH promoter in GT1-7 cells. As expected, the wild-type (WT) GnRHe/p reporter was significantly activated in response to Six6, Otx2 and Dlx5. However, neither Six6 nor Dlx5 were able to activate the mutant reporter (E+P Del), indicating that both factors function through these four homeodomain binding sites to regulate GnRH promoter activity. Importantly, deletion of the ATTA sites had no effect on the ability of Otx2 to significantly induce reporter activity because its primary site of action is via a bicoid-like target sequence within the GnRH promoter at -152 bp (Kelley, 2000; Larder, 2009). Interestingly, the ability of Msx1 to significantly repress GnRH promoter activity was not compromised by the mutation of these four ATTA sites, likely due to the fact that Msx1 can regulate GnRH expression via interactions with other modulators of GnRH transcription such as Oct-1 (Givens, 2005).

To determine whether the activity of Six6 was dependent on the presence of all four ATTA sites, or just those in either the promoter or enhancer, deletions in either the two promoter sites (P Del) or the two enhancer sites (E Del) were generated and the transient transfection assays repeated. Dlx5 was capable of activating both the E Del and P Del mutant reporters indicating that all four ATTA sites are required for maximal induction of the GnRH promoter by this transcription factor (Fig. 1.10*C*). Interestingly, Six6 was only able to significantly activate the enhancer-deleted reporter demonstrating that the primary site of Six6 action is via the ATTA sites situated within the conserved, proximal promoter.

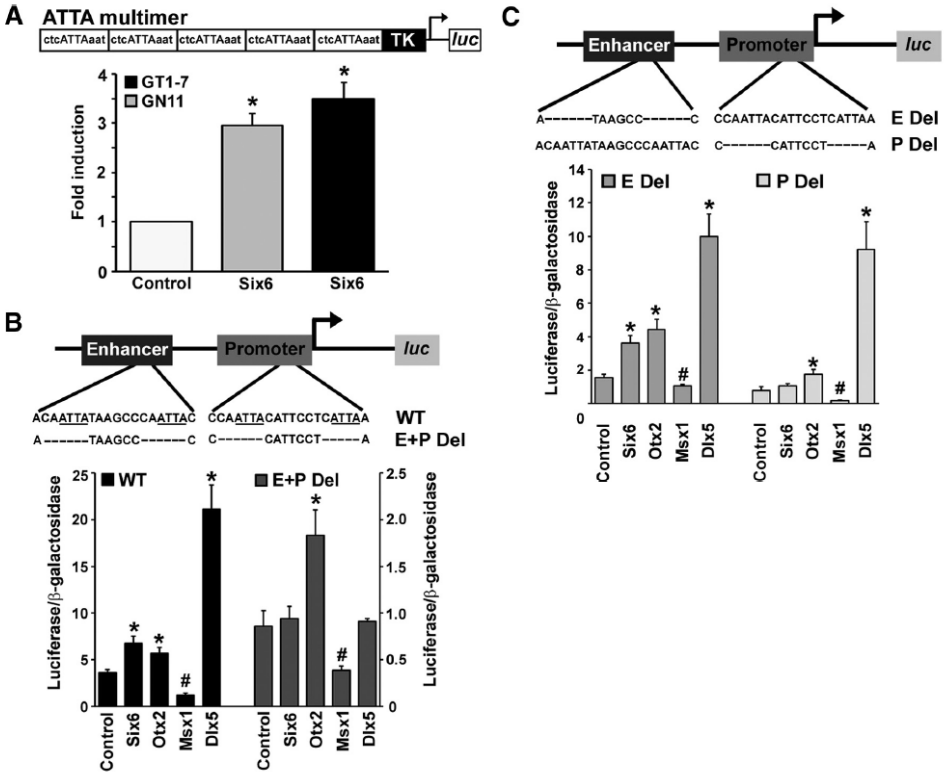

Figure 1.10. The primary site of Six6 activation is via promoter ATTA sites. ***A****,* Effect of over-expression of Six6 on ATTA-multimer in GN11 and GT1-7 cells. Thymidine kinase (TK); luciferase (luc). Fold-induction compared to 'empty' vector alone (control) is indicated, corrected for β-galactosidase, which was used as an internal control. Over-expression of Six6 resulted in significant fold induction of an ATTA-multimer in both cell lines. All experiments were performed in triplicate and repeated three times. Results shown are average ± SEM. One-way ANOVA established statistical significance of Six6 expression plasmid vs. 'empty' expression plasmid (control) as '*', $p<0.05$. ***B****,* Six6 expression plasmid was co-transfected into GT1-7 cells with either a wild-type GnRHe/p reporter (WT) or a mutant GnRHe/p reporter (E+P Del) where all four ATTA sites (underlined in WT) have been deleted ('-' in mutant). The left axis shows luc/βgal values for the WT reporter, the right axis shows the luc/βgal values for the E+P del reporter. ***C****,* Six6 expression plasmid was co-transfected into GT1-7 cells with mutant GnRHe/p reporters where either the two enhancer ATTA sites (E Del) or the two promoter ATTA sites (P Del) are deleted. Results shown are average ± SEM. All experiments were performed in triplicate and repeated three times. One-way ANOVA with *post hoc* Tukey test established statistical significance as $p<0.05$. '*' represents significant activation vs. empty vector 'control'. '#' represents significant repression vs. empty vector 'control'.

Chapter 1.4: Discussion

As the key regulator of reproduction, correct expression of GnRH is crucial to achieving appropriate reproductive function. Understanding the factors and mechanisms that control the synthesis and release of GnRH are vital to understanding fertility. Herein we identify a member of the sine oculis homeobox (Six) family of transcription factors as an important, novel regulator of mammalian fertility. Our data show that loss of Six6 expression leads to significantly decreased fertility in both male and female mice, due to disrupted regulation of GnRH expression.

While progress has been made in identifying gene targets of Six1-5 (Brodbeck, 2004; Harris, 2000; Laclef, 2003; Ozaki, 2004; Spitz, 1998), little is known about the function of Six6 other than its role as a stimulator of progenitor cell proliferation in the developing pituitary and eye (Li, 2002). Therefore, we were intrigued to identify Six6 as one of the most differentially regulated transcripts from a microarray comparison of immature (GN11) and mature (GT1-7) GnRH neuronal cell lines [(Miller, 2009) and unpublished data]. The observed ~180 fold increase in Six6 expression correlated with a ~130 fold increase in GnRH expression implicating Six6 as an important regulator of GnRH gene expression. This novel role for Six6 was confirmed by experiments demonstrating that over-expression of Six6 in two GnRH neuronal cell lines significantly increased GnRH transcription and this increase was mediated via Six6 binding to ATTA sites within the GnRH proximal promoter. We previously reported the importance of these sites in the regulation of GnRH expression and showed that they can bind other homeodomain-containing transcription factors such as Msx1/2 and Dlx1/2/5 (Givens, 2005). Our data suggest that while Dlx5-mediated activation of GnRH transcription can occur via all four ATTA

sites, the primary sites of Six6 action are the ATTA elements located within the rat GnRH proximal promoter at -41 and -53 bp. While Six6 is capable of binding to all four ATTA sites, only deletions involving the two promoter sites result in loss of GnRH induction in response to Six6. This suggests that cooperation between Six6 and other factors that bind at, or near, the promoter ATTA sites, may play a role in allowing maximal activation of GnRH transcription. Six3 has been shown to function as a context-dependent activator (Liu, 2006) or repressor (Lagutin, 2003; Zhu, 2002) in both the developing eye and forebrain, suggesting that its function is dependent on its interaction with specific co-factors. To our knowledge, this is the first report to detail activation of gene transcription by Six6. Previous studies using yeast two-hybrid screens, with Six6 as the bait, yielded members of the Groucho family of co-repressors as potential Six6 interacting partners (Lopez-Rios, 1999), however no co-activators have been identified by this screening method. Further investigation is warranted to establish whether Six6 acts alone, or in co-operation with other factor(s) to induce GnRH gene expression.

Based on the expression profile of Six6 in the GnRH neuronal cell lines, and its ability to activate GnRH transcription, we sought to determine the reproductive phenotype of mice lacking expression of Six6. Both male and female Six6-null mice had significantly reduced fertility, reinforcing our hypothesis that Six6 is important for proper neuroendocrine control of reproduction in mammals. The presence of antral follicles in KO ovaries, along with the absence of CL, strongly implicates LH deficiency as the primary cause of infertility in female animals. Immunohistochemical analysis of pituitaries from these mice revealed comparable numbers of LHβ-expressing gonadotrope cells, suggesting that gonadotrope function is not

altered, but rather that the hypothalamic signal to the pituitary is disrupted. This hypothesis was corroborated by the observation that Six6-null females have significantly lower levels of GnRH mRNA and 89% fewer GnRH neurons. Therefore, it is likely that the anovulatory phenotype seen in Six6-null females is because the decreased numbers of GnRH neurons are insufficient to generate a GnRH/LH surge. Indeed, previous studies have shown that female mice require 12-34% of the normal GnRH neuronal population to ensure the generation of an effective GnRH/LH surge (Herbison, 2008). Characterization of the reproductive phenotype of Six6-null males reveals a similar 84% decrease in GnRH neuron numbers and confirms previous studies showing that pulsatile secretion of LH in male mice is achievable with only a few GnRH neurons. Furthermore, our results support data that demonstrates a differential effect of reduced GnRH neuron numbers on plasma gonadotropin levels in males (Gibson, 1997; Herbison, 2008). Six6 KO males have a much greater reduction in serum FSH concentrations (~75%) than either LH or T (~35%), suggesting that a larger cohort of GnRH neurons is required to maintain normal levels of FSH in males.

At e13.5, Six6-null mice have comparable numbers of GnRH neurons to their WT littermates. Nevertheless GnRH neuron numbers are decreased at birth mirroring a similar phenotype to that seen in NSCL-2-null mice (Kruger, 2004). Given that vaginal opening is not delayed in Six6-null females, this signifies that, as observed in GNR23 mutant mice, typical pubertal advancement can occur even with only a handful of GnRH neurons (Gamble, 2005; Herbison, 2008). However, normal development of the GnRH neurons in Six6-null mice is perhaps not surprising given the very low levels of Six6 expression in immature GnRH neuronal cells. Assuming Six6 expression is low in immature GnRH neurons *in vivo*, then loss of Six6

expression during embryonic development would likely have a negligible impact on GnRH neuronal migration. Moreover, expression of Six3 during development may compensate for the loss of Six6 at early stages of GnRH neuronal biology as both factors induce GnRH promoter activity in an immature GnRH neuronal cell line. However, further investigation of the role of Six3 during GnRH development is required to confirm this hypothesis.

Unlike Six6-null mice, Six3 knock-outs die at birth (Lagutin, 2003), so it is not possible to assess the reproductive phenotype of these animals. While both sub-group family members activate GnRH promoter activity in immature GnRH neurons, they have differential actions on GnRH transcription in a mature GnRH neuronal cell line. Six6 induces GnRH transcription in GT1-7 cells, whereas Six3 represses it. However, the repressive effects of Six3 are reversed by titrating in increasing amounts of Six6. Quantitative analysis of Six3 and Six6 expression levels reveals that Six3 is expressed similarly in both cell models, whereas Six6 expression is increased ~200-fold as the GnRH neuron matures, resulting in 10x the amount of Six6 as Six3 in the GT1-7 cells. Therefore, our titration experiment mirrors the changes seen in the relative expression levels of the two factors and suggests that once a critical level of Six6 expression is achieved then activation of the GnRH promoter will be favored. We hypothesize that the substantial decrease in GnRH mRNA and protein levels observed in Six6-null mice may be due to the lack of Six6 expression not only affecting induction of GnRH transcription but also allowing the repressive actions of Six3 on the GnRH promoter to be fully realized.

Both Six6 and Six3 have also been shown to be expressed in the developing (Jean, 1999; Oliver, 1995) and adult pituitary (Aijaz, 2005), and, while it is unknown

whether both factors are expressed in all six anterior pituitary cell-types, our unpublished observations indicate both are expressed in two immortalized gonadotrope cell lines (LβT2 and αT3-1 cells). However, GnRH-challenge experiments performed in male Six6-null mice reveal that KO pituitaries respond to GnRH in an identical manner to WT pituitaries, suggesting that loss of Six6 expression does not affect the ability of the pituitary to respond to GnRH, but rather that the fertility defects seen in these animals are due to disruption at the apex of the HPG axis. Our data reveal that the hypothalamic effects of deleting Six6 are not confined to the GnRH neuronal population. Disruption of kisspeptin neurons also causes infertility (Clarkson, 2008), however, the reduction in GnRH neurons in Six6-null mice is likely to be the main cause of infertility. Detailed characterization of a GnRH-neuron specific knock-out of Six6 would confirm this and determine the reproductive contribution of Six6 expression in other neuronal populations. Defects in GnRH cell fate specification, differentiation, migration, axonal elongation, and targeting to the median eminence can all contribute to deficiencies in GnRH secretion, which results in the clinical syndromes known as idiopathic hypogonadotropic hypogonadism (IHH) and Kallmann's syndrome (Bianco, 2009). Given that loss of Six6 expression has such a dramatic effect on GnRH expression in mice, and that genetic mutations have only been identified in ~30% of IHH patients (Pitteloud, 2007), it will be important to determine whether *SIX6* mutations are observed in cases of IHH of unknown genetic etiology.

In conclusion, we have identified Six6 as an important hypothalamic regulator of fertility in mice. Lack of Six6 results in a decrease in GnRH gene expression, reduced numbers of GnRH neurons and decreased targeting of GnRH neurons to the

median eminence, leading to infertility in adult mice. We, therefore, hypothesize that mutations in SIX6 may contribute to cases of hypogonadotropic hypogonadism and infertility in humans.

Chapter 1 is a reprint of material appearing in the Journal of Neuroscience 2011. Larder, Rachel; Clark, Daniel; Miller, Nichol; Mellon, Pamela. “Hypothalamic Dysregulation and Infertility in Mice Lacking the Homeodomain Protein Six6.” Journal of Neuroscience, 2011 Jan 12; 31(2):426-38. This paper was written by Rachel Larder; the dissertation author was the second author of this paper.

Chapter 2: Six6 is Required for the Development of the Suprachiasmatic Nucleus and Circadian Rhythms

Chapter 2.1: Introduction

The suprachiasmatic nucleus (SCN) of the mammalian hypothalamus is a central pacemaker of circadian rhythms. Physical ablation of this nucleus in rodents leads to behavioral arrhythmicity (Stephan, 1972) and impaired fertility (Wiegand, 1982). Light input from photosensitive retinal ganglion cells in the eye entrains the SCN's approximately 24 hr activity patterns to advance or delay the phase of rhythm such that the physiology of the animal is appropriately timed to its environmental context (Panda, 2002).

Six6, a murine homeobox gene orthologous to *Drosophila optix* (Jean, 1999), has been shown to play important roles in the developing eye, brain, and pituitary. It is expressed as early as 8 days post conception in the mouse. Throughout development, it is expressed in the hypothalamus, the pituitary, and the olfactory placode, and is later expressed in the optic vesicle, the optic stalk, and the retina (Jean, 1999). In adult, it remains expressed in the hypothalamus as well as cells of the eye, and the pituitary [GeneAtlas record GSE10246 (MOE430.gcrma)]. Deletion of the mouse Six6 gene leads to defects in precursor cell proliferation in the retina and the pituitary (Li, 2002).

Six3 is a close homolog of *Six6*, and the two share partially overlapping expression patterns (Jean, 1999). *Six3* and *Six6* were among several transcription factors recently identified as being expressed early in development and strongly in the postnatal suprachiasmatic nucleus (Vandunk, 2011). Neuronal deletion of *Six3* was accomplished by breeding a floxed *Six3* allele-bearing mouse line (Liu, 2006)

with a mouse line expressing Cre recombinase under the control of a neuron-specific enhancer from the *Nestin* gene (Tronche, 1999). Mice with complete neuronal deletion of *Six3* had no SCN. This was in contrast to the presence of normal SCN in mice lacking functional *RORα* (Hamilton, 1996), a gene also expressed strongly in the SCN and early in development.

Recently, *Six6* was shown to play a critical role in reproduction (Larder, 2011). Gonadotropin-releasing hormone- (GnRH-) secreting neurons in the hypothalamus control the pituitary gonadotrope cells that, in turn, control reproduction. In a screen to identify genes important for GnRH neuron function, *Six6* was found to be over one hundred-fold upregulated in a cell model (GT1-7 line) of a mature GnRH neuron compared to a cell model (GN11 line) of an immature GnRH neuron. Female mice lacking *Six6* showed a profound infertility phenotype; only one knock-out female out of an experimental cohort of eight was able to deliver a single litter over three months. Also, both male and female *Six6* knock-out mice had significantly reduced numbers of GnRH neurons. However, an altered pattern of tyrosine hydroxylase expression in the hypothalamus suggested a more general role for Six6 in the development of the hypothalamus.

Given the developmental and spatial expression pattern of *Six6* and role of its homolog *Six3* in the formation of the SCN, interesting questions remain concerning the role of *Six6* in the brain. Do mice lacking *Six6* also lack SCN, as observed in the neuron-specific *Six3-null* mice, or are the SCN of *Six6-null* mice intact, as observed for the *RORα* mice? We first characterized the temporal expression pattern of *Six6* in the adult hypothalamus, and then characterized the circadian behavioral phenotypes of *Six6* knock-out mice. The suprachiasmatic nucleus of the *Six6* knock-out mouse

was then characterized using immunohistochemical staining for the SCN markers arginine vasopressin (AVP) and vasoactive intestinal polypeptide (VIP).

Chapter 2.2: Materials and Methods

Animals and housing. *Six6*-null (*Six6*-/-) mice were obtained from Dr. Xue Li (Children's Hospital of Boston, Harvard Medical School, Boston, MA), and were maintained in accordance with protocols approved by the University of California, San Diego Institutional Animal Care and Use Committee. Animals were housed under 12h:12h light:dark lighting conditions, except as noted below, and were given *ad libitum* access to food and water. Our colony was maintained on a mixed 129/Sv (original) and C57BL/6 (3 generation backcross) background strain.

Q-RT-PCR. Male mice heterozygous for the *Six6* deletion allele were euthanized at zeitgeber time 20 (ZT20), four hours prior to lights on (in the dark, n = 4) and at ZT8, four hours prior to lights off (n = 4). Hypothalami were dissected and transferred to Trizol reagent (Life Technologies; Carlsbad, CA). RNA was extracted according to the manufacturer's instructions. cDNA was prepared using a SuperScript III first-strand cDNA synthesis kit (Life Technologies). Quantitative PCR was performed using a BioRad (Hercules, CA) iQ5 system and B-R-SYBR Green (Quanta Biosciences; Gaithersburg, MD). Gene-specific PCR primers (Table 2.1) were used to determine the expression levels of mouse *Six3*, *Six6*, *Bmal* (*Arntl*), and *Per2*, along with the control genes *Gapdh*, *H2afz*, and *Ppia*. Known quantities of reference DNA plasmids each containing a gene of interest were used to prepare standard curves, against which the hypothalamic expression levels were measured. Expression of

each gene of interest was normalized to the geometric average of the expression of the three control genes at each time point (Vandesompele, 2002).

Table 2.1. PCR primer DNA oligonucleotides.

Gene Symbol	Accession	Primer	Sequence (5' to 3')
Six6	NM_011384.4	Six6_F	TCGATGTTCCAGCTGCCCAT
Six6	NM_011384.4	Six6_R	TGGAAAGCCACGATGGCTCT
Six3	NM_011381.4	Six3_F	CCGGAAGAGTTGTCCATGTT
Six3	NM_011381.4	Six3_R	CGACTCGTGTTTGTTGATGG
Arntl	NM_007489.3	Bmal1_F	ATTCCAGGGGGAACCAGAG
Arntl	NM_007489.3	Bmal1_R	CCCTCCATTTAGAATCTTCTTGC
Per2	NM_011066.3	Per2_F	CAAAGGCACCTCCAACATG
Per2	NM_011066.3	Per2_R	AAAGTATTTGCTGGTGTGACTTG
Gapdh	NM_008084.2	GapDH_F	TGCACCACCAACTGCTTAG
Gapdh	NM_008084.2	GapDH_R	GGATGCAGGGATGATGTTC
Ppib	NM_011149.2	CycB_F	CGTGGCCAACGATAAGAAGA
Ppib	NM_011149.2	CycB_R	GAAGTCTCCACCCTGGATCA
H2afz	NM_016750.2	H2afz_F	TCACCGCAGAGGTACTTGAG
H2afz	NM_016750.2	H2afz_R	GATGTGTGGGATGACACCA

Photoperiod manipulations. *Six6*-/- mice (n=6) and wild-type littermate controls (n=6) were raised in a 12:12 light:dark photoperiod until two to four months of age. Mice were then introduced into cages containing running wheels equipped with magnets and monitored using magnetic switches. All cages were contained within a light-tight cabinet with programmable fluorescent lighting. The previous photoperiod was maintained, and the mice were given seven days to acclimate to the new environment. Wheel turns were recorded for each mouse in 6 minute bins and analyzed offline using the Clocklab (Actimetrics; Wilmette, IL) suite of Matlab

(Mathworks; Natick, MA) plugins. Actograms were plotted using the above software, Mircosoft Excel, and an online plotting program produced by Roberto Refinetti (http://www.circadian.org/actogram.html, accessed 2011). Four different photoperiod manipulations were performed: 1) a 12h:12h light:dark schedule, 2) complete darkness, 3) a 1:11 L:D skeleton photoperiod, and 4) a 6:6:6:6 L:D:L:D, bifurcated light schedule.

Hypothalamic immunohistochemical staining. Mice were cardiac-perfused with a phosphate-buffered saline (PBS) solution followed by a 4% formalin solution of PBS. Brains were dissected from the skull and post-fixed for 16 hours in a 4% formalin PBS solution. Brains were then transferred to a 50% sucrose solution of PBS for 12 hours and then embedded in O.C.T. compound (Tissue-Tek; Sakura Finitek USA; Torrance, CA) and frozen at -80°C. Brains were sectioned at 20 μm and thaw-mounted onto PermaFrost plus glass slides. Slides were stained using one of three primary antibodies: polyclonal rabbit anti-VIP (ImmunoStar; Hudson, WI), rabbit anti-vasopressin (ImmunoStar), or rabbit anti-tyrosine hydroxylase (Pel-Freez; Rogers, AR). Slides were then processed and stained with a peroxidase substrate chromogen kit (Vector VIP; Vector Labs; Burlingame, CA) according to the manufacturer's recommendations.

Chapter 2.3: Results

Diurnal expression pattern of *Six6*. While the developmental and spatial expression pattern of *Six6* has been reported in the mouse (Vandunk, 2011), its expression in the SCN over circadian time is not known. We used Q-RT-PCR to measure the expression levels of *Six3* and *Six6* at two zeitgeber time points. The two

time points chosen were near the expected times of maximal and minimal expression of genes known clock genes *Bmal* and *Per2*. These time points are also near the times of maximal and minimal expression of *Six3* (Vandunk, 2011). At ZT8, the hypothalamic expression of *Bmal* is significantly lower and expression of *Per2* is significantly higher than their expression at ZT20 (Fig. 2.1). Expression of *Six3* is significantly lower at ZT20 than at ZT8, and this finding is consistent with a previous report (Vandunk, 2011). *Six6* expression was significantly lower at ZT20 than at ZT8, indicating that *Six6* expression is also diurnally regulated (Fig. 2.1).

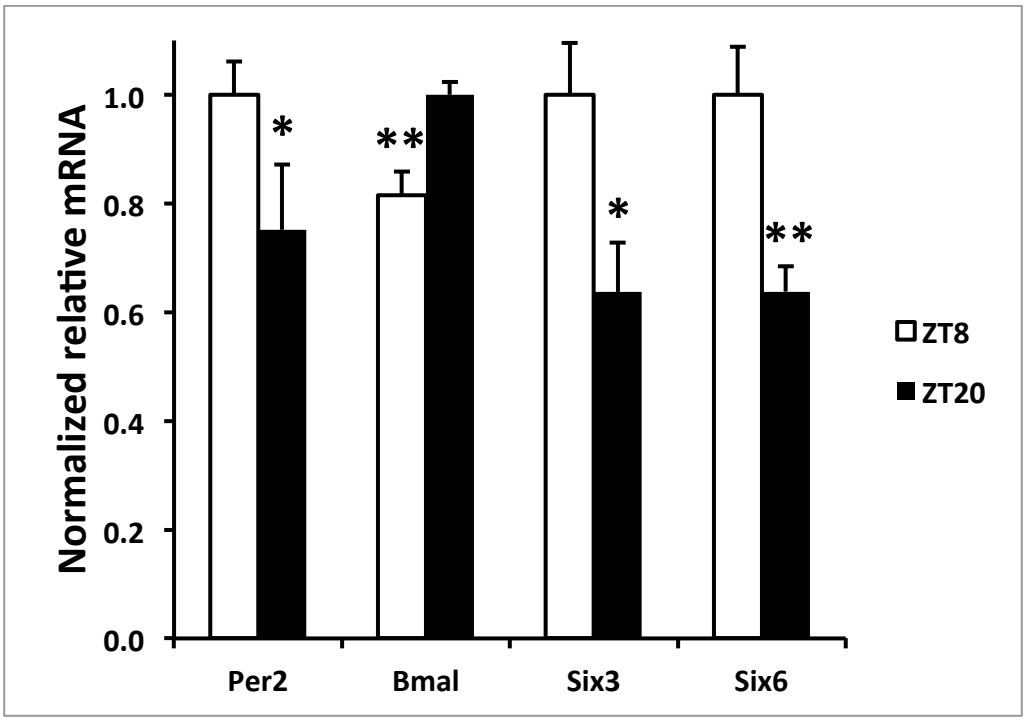

Figure 2.1. Hypothalamic gene expression at two points in circadian time. Gene expression data obtained via Q-RT-PCR. Each gene's expression has been normalized to the geometric mean of three control genes (see Materials and Methods), and is expressed relative to the peak average value between the two groups, ZT8 (n = 4) and ZT20 (n = 4). Single asterisk indicates a statistically significant difference in expression ($p \leq 0.05$ via Student's t-test) between the ZT8 and ZT20 groups for each gene; double asterisk indicates $p \leq 0.01$.

Abnormal light entrainment of the *Six6* knock-out mouse. Wild-type mice entrained normally to the 12:12 photoperiod, as assessed from their wheel running activity (Fig. 2.2). WT mice showed robust wheel-running during the dark portion of the photoperiod, and almost complete absence of activity during the light portion of the photoperiod (masking). *Six6*-/- mice showed a variety of entrainment activity patterns. Two of the *Six6*-/- mice showed nearly normal entrainment to the L:D photoperiod (Six6 KO B, Fig. 2.2). Other *Six6*-/- mice showed greater activity during the dark portion of the photoperiod than the light portion, but the activity bouts did not show the characteristic sharp onset and gradual offset of activity during the dark—rather, there appeared to be two separate bouts of activity following lights off and prior to lights on (Six6 KO A). Two of the six *Six6*-/- mice did not appear to have any differences in wheel running behavior between light and dark portions of the photoperiod (Six6 KO C).

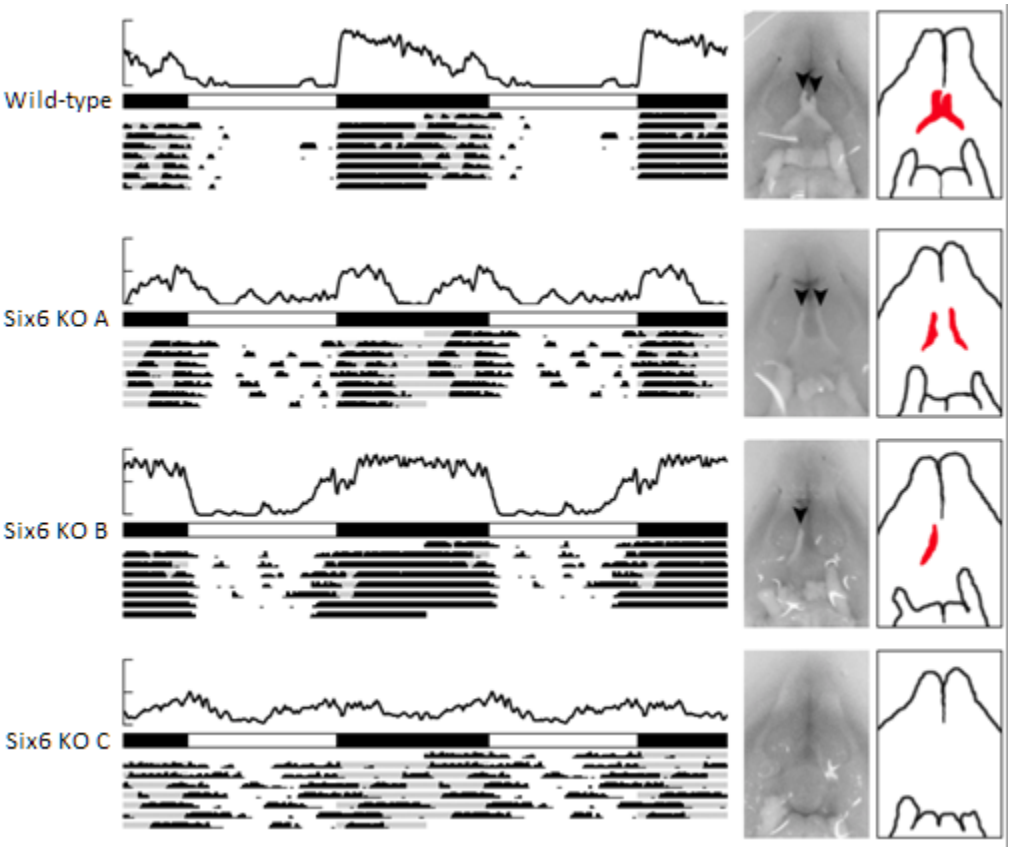

Figure 2.2. Wheel running activity and optic nerve phenotypes of four mice. For each mouse, an average activity plot (top; y-axis maximum = 1000 revolutions per 6 minutes) is shown above actograms representing seven days of wheel running data (each actogram is double plotted such that 48 hours of data are shown for each row). To the right of the activity are photographs and schematic drawings of each mouse's optic nerve phenotype. The ventral surface of each brain is shown, with the location of the optic nerve centered. Black arrowheads represent the presence of optic nerves.

Variable optic nerve phenotype in *Six6*-/- mice. The presence of the optic nerve is variable in *Six6*-/- mice (Li, 2002). Wild-type and KO animals were sacrificed and dissected. As the brain was dissected out, care was taken to note the size and presence of each optic nerve. Wild-type mice had normal optic nerves, but *Six6*-/- mice had one of three optic nerve phenotypes. Half of the *Six6*-/- mice studied (n = 7/14) had no optic nerve, or thread-like, severely atrophied or poorly developed optic nerves, with no visible optic chiasm. Interestingly, the eyes of these knock-out mice appeared relatively normal, with no obvious atrophy or lid closure. A second phenotype (n = 5/14) of *Six6*-/- mouse was characterized by the presence of either the right or the left optic nerve, with the other completely missing. A third *Six6*-/- phenotype (n = 2/14) was characterized by the presence of both optic nerves, but a lack of chiasm. In these mice, the optic nerves appear to project straight back to the thalamus. It is unclear whether all or some of the retinohypothalamic tract (RHT) is missing in these mice. The photoperiod entrainment of the *Six6*-/- mice seemed to depend on the optic nerve phenotype. This raises the interesting hypothesis that the SCN of these mice is similarly variable.

Abnormal free-running activity of the *Six6* knock-out mouse. Following photoperiod entrainment, wild-type and knock-out mice were released into constant darkness. With no environmental cues indicative of day length, wild-type mice (n = 6) retained robustly rhythmic activity patterns with a period of $\tau = 23.7 \pm 0.16$ hours. However, *Six6*-/- mice displayed a range of activity patterns in constant darkness (Fig. 2.3). *Six6*-/- mice with single or double intact optic nerves showed a range of free-running activity patterns, with some showing strong circadian periodicity (n = 3, $\tau = 24.40 \pm 0.50$), and one showing weak circadian periodicity (multiple weak chi-

squared periodogram peaks; Six KO B from Fig. 2.3). Neither of the two *Six6*-/- mice without optic nerves had strong circadian rhythms, but one had strong ultradian periodicity (FFT peak = 6.40 hrs, relative power = 0.12, Fig. 2.3) and the other had weak ultradian periodicity (FFT peak = 7.00 hrs, relative power = 0.04).

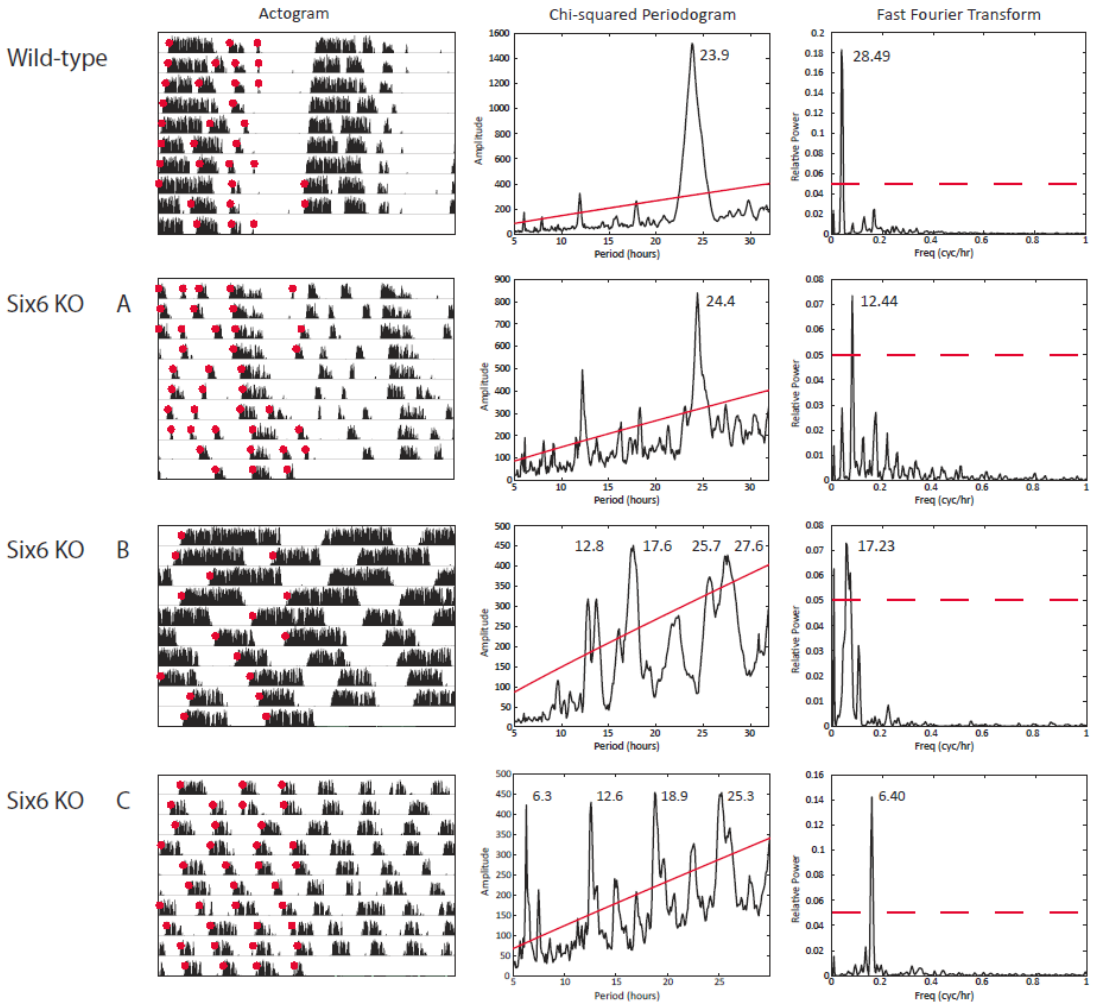

Figure 2.3. Wheel running activity during constant darkness. Left) Wild-type and knock-out mouse wheel running actograms are shown for 10 days of activity. Middle) Chi-squared periodogram analysis of the actogram data. Diagonal line represents 0.05 significance threshold. Right) Fast Fourier transform of the actogram data. Peak period listed; dotted line represents 0.05 relative power. Knock-out mice A, B, and C are the same mice as in Figure 2.2.

Abnormal skeleton photoperiod activity of the *Six6* knock-out mouse. Given the abnormal and variable activity patterns of the *Six6*-/- mice during standard 12:12 photoperiods and under constant darkness, we subjected wild-type and *Six6*-/- mice to two additional alternative photoperiods. Rodents are capable of entraining to brief, one hour pulses of light given every twelve hours (Pittendrigh, 1976). Robust activity is typically consolidated between two of these pulses (subjective night), and a period of inactivity is consolidated between the other two (subjective day). Wild-type and *Six6*-/- mice were subjected to these skeleton photoperiods in order to determine whether *Six6*-/- mice display subjective day and night wheel-running activity. Wild-type mice behaved as expected with six out of the six WT mice displaying subjective night and subjective day activity patterns (Figs. 2.4 and 2.5). The activity patterns of three out of the four knock-out mice with at least one optic nerve suggested that there was no subjective day or night for the KO mice—their activity was distributed equally between the light pulses, unlike the wild-type activity. The KO mice with no optic nerve continued to essentially free-run.

Because *Six6-/-* mice showed an apparent decrease in the ability of light to mask wheel-running activity relative to wild-type mice, we subjected wild-type and *Six6-/-* mice to a bifurcated, 6:6:6:6, L:D:L:D photoperiod to investigate whether the effects of masking would be different with an increased frequency of dark onset. *Six6*-/- mice showed similar behavior to wild-type mice in a bifurcated photoperiod. *Six6*-/- mice in a bifurcated photoperiod with four light/dark transitions per 24 hr showed strong activity during the dark portion of the photoperiod, as did wild-type mice (Fig. 2.4).

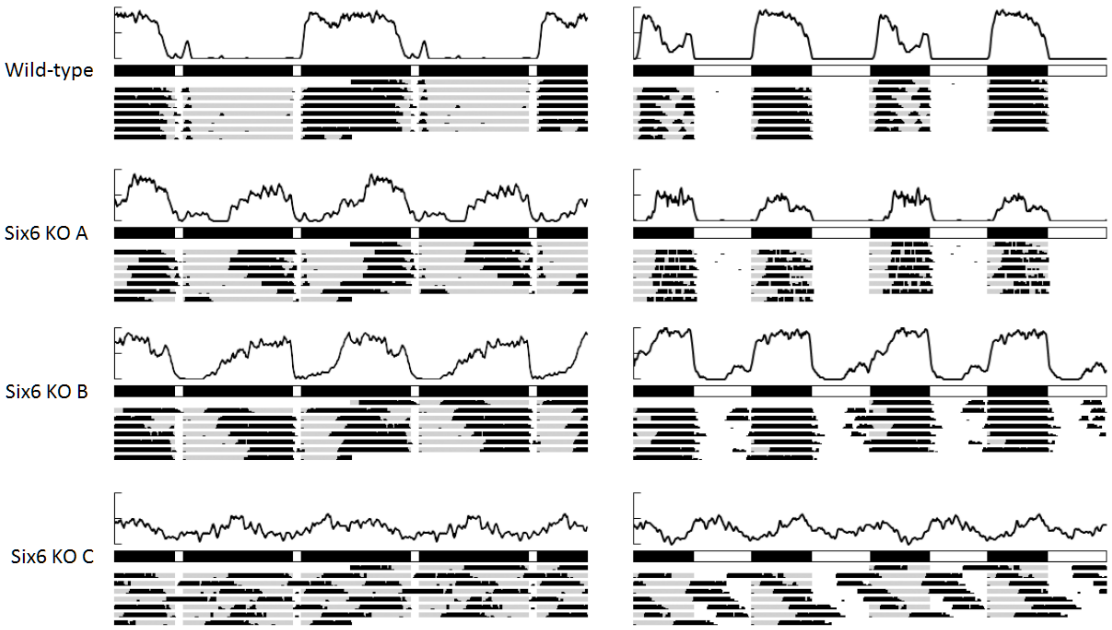

Figure 2.4. Wheel running activity during skeleton and bifurcation photoperiods. Left) Wild-type and knock-out mouse average activity (top) and actogram (bottom) during seven days of activity in a skeleton photoperiod of 1:11 L:D. Right) Wild-type and knock-out mouse average activity (top) and actogram (bottom) during seven days of activity in a bifurcated 6:6:6:6 L:D:L:D photoperiod. As in Figure 2.2, each activity average and actogram is double plotted over 48 hours of activity. Knock-out mice A, B, and C are the same mice as in Figures 2.2 and 2.3.

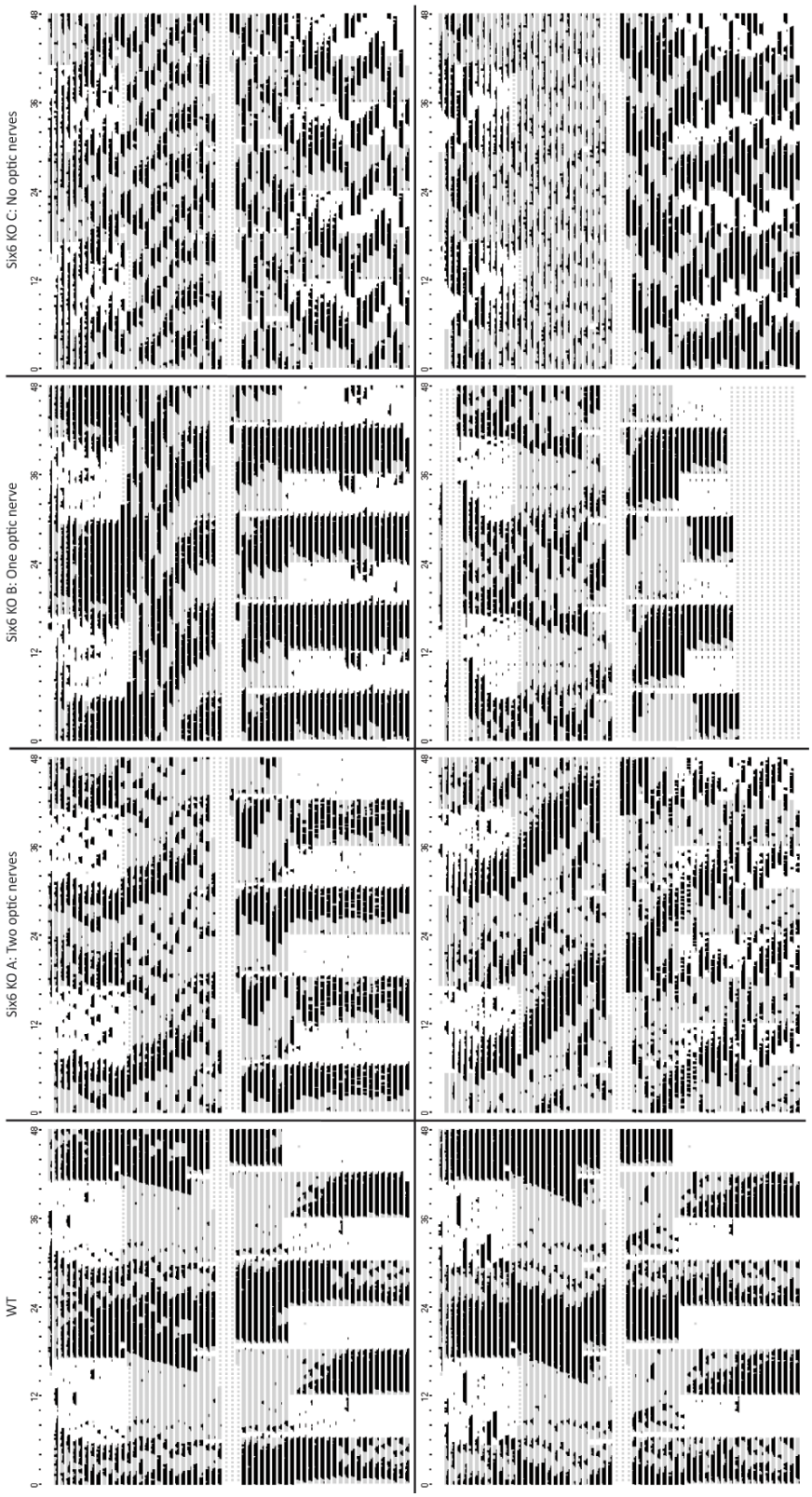

Figure 2.5. Full activity profile of six Six6 KO and two WT mice. Shaded background indicates dark portions of the photoperiod. Dotted gray lines indicate missing data.

Six6 knock-out mouse SCN phenotype. The mouse SCN is characterized by a VIP-positive core region at its ventral base, and an AVP-positive shell region surrounding the core dorsally. Staining for these two proteins has been used extensively to characterize the SCN (Leak, 2001). Wild-type and the three types of *Six6* KO mouse hypothalami were sectioned and stained for these markers as described in the Materials and Methods section (Fig 2.6). Given that the range of circadian phenotypes varied along with optic nerve phenotypes, we hypothesized that the SCN of *Six6*-/- mice would similarly vary. However no *Six6*-/- mouse, regardless of optic nerve phenotype, had SCN. All WT mice had discrete, bilateral SCN morphologically identifiable through the dense ventral hypothalamic region of small cell bodies characteristic of the SCN, prominent following TH staining. No *Six6*-/- mice showed such nuclei. Via direct staining for the SCN markers AVP and VIP, no *Six6*-/- mice showed SCN. However, as described previously for the conditional *Six3*-/- mice, other hypothalamic nuclei with AVP-positive neurons [e.g. the supraoptic and paraventricular nuclei (Vandunk, 2011)] were present in *Six6*-/- mice (Fig. 2.6). Interestingly, the AVP-positive supraoptic nuclei are present in *Six6*-/- mice lacking optic nerves. The absence of SCN in *Six6*-/- mice of all optic nerve phenotype indicates that the role *Six6* plays in the development of the SCN is not secondary to the defects seen in the optic nerve. *Six6* itself is required for the development of the SCN.

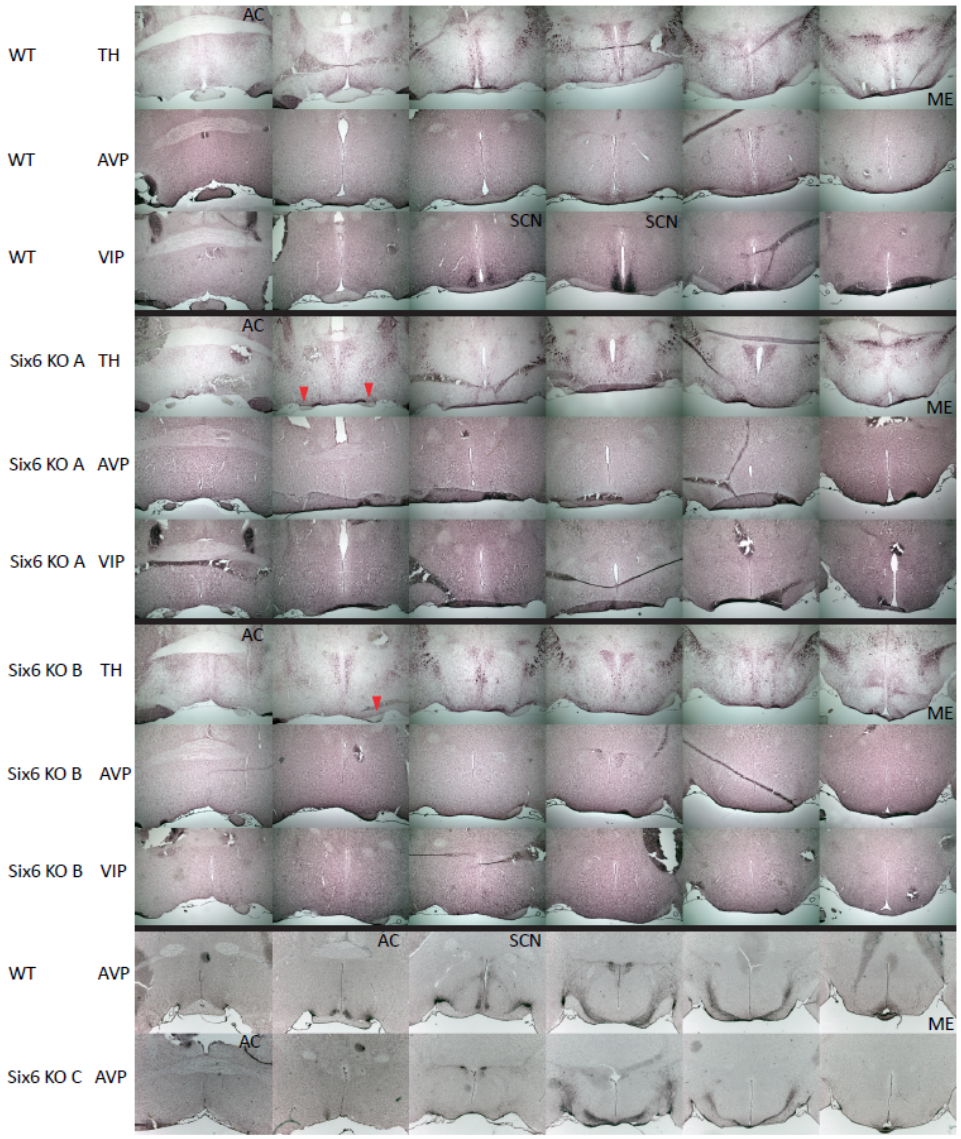

Figure 2.6. SCN of wild-type and Six6 knock-out mice. WT and KO mouse hypothalamic coronal brain sections stained for TH, AVP, and VIP (see Materials and Methods). Upper nine rows of images were stained in one batch with identical conditions except for primary antibody. Lower two rows of images were stained with a different lot of AVP antibody than the upper rows. Each leftmost column of images is of the rostral hypothalamus, approximately at the level of the anterior commissure (AC). Each rightmost column of images is of the caudal hypothalamus, approximately at the level of the median eminence (ME). Red arrowheads indicate optic nerve (ON) locations in KO mice A (two ON) and B (single ON). In none of the KO mice could SCN be identified directly by AVP or VIP staining or by indirect morphological evidence by TH staining. All WT mice examined displayed normal SCN via all three methods.

Chapter 2.4: Discussion

The developmental origins of the mouse SCN have been examined using BrdU labeling (Kabrita, 2008), as well as transcription factor profiling (Vandunk, 2011). Beginning around embryonic day 12 (Kabrita, 2008), the first cells of the SCN undergo terminal differentiation in the core region that will eventually become VIP-positive. On embryonic days 13.5-14, the cells of the shell terminally differentiate. This developmental process likely shares many of the general principles of neurodevelopment, with transcription factors, signaling events, and environmental cues playing a role.

Prior to the birth of the earliest SCN cells, the retinal ganglion cells send their axons (embryonic day 13) to their thalamic targets (Hinds, 1974; Lund, 1976). However, the retinohypothalamic tract does not innervate the rat SCN until after birth (Mason, 1977; Stanfield, 1976), well after the SCN has formed and begun expression of the markers VIP and AVP. Since the formation of the optic nerves precedes the formation of the SCN—and lies in such close proximity to it—the SCN may in some part rely on signaling from the optic nerves for its formation. The variability of the *Six6*-/- mouse optic nerve phenotype may provide an avenue to test this.

In rodents blinded via orbital enucleation, the morphology of the SCN is altered. In rats enucleated (bilaterally or unilaterally) at four weeks of age, the optic chiasm becomes thinner, SCN is displaced rostrally, and the number of cells in the typical location of the SCN is decreased (Nagai, 1992). However, the overall number of cells in the SCN was not affected by enucleation. The enucleation experiments were performed in rats at four weeks of age, and thus reflect changes to the SCN after its initial development.

Previous work on transgenic and mutant mouse lines has explored the retinohypothalamic tract and its role in SCN development and physiology. Early work on the *eyeless* mouse [strain ZRDCT-AN (Chase, 1941), later confirmed to possess a single nucleotide polymorphism removing an alternate start codon of the *Rx/rax* gene (Tucker, 2001)] revealed hypothalamic and optic tract deficiencies (Laemle, 2002; Silver, 1977) in these mice. The SCN of the *eyeless* mouse strain is variably atypical, with 70% showing normal SCN morphology and cell densities, and the remaining mice showing laterally asymmetric deficiencies in SCN size and cell number (Silver, 1977). Seventy-five percent of anopthalmic mice studied (Laemle, 1998) showed stable circadian activity rhythms, 10% showed unstable rhythms, and 15% were behaviorally arrhythmic. In contrast to the *Six*-/- mice reported here, the anopthalmic arrhythmic mice did not show any predominant ultradian periodicity. Whether the SCN and behavioral phenotype are due to developmental stochasticity or due to multifactorial inheritance of this polygenic trait is unknown, but this phenotypic variability is shared with the *Six*-/- mice.

The SCN phenotype in *Six*-/- mice is not likely due to a lack of RHT input to the SCN. In an “RHT knock-out” model, mice lacking rod and cone cells and the *melanopsin* gene (*Opn4*) display robust circadian rhythmicity, though this rhythmicity is not entrainable by light (Panda, 2003). From *in utero* through adulthood, these mice have had no retinal input to the SCN, suggesting that this input is not necessary for SCN development and function. The optic nerves and optic chiasm in these mice, however, are intact.

The activity patterns of the *Six6*-/- mice share some similarity to the activity patterns of mice in which the genes for VIP and peptide histidine leucine (PHI) were

deleted (Colwell, 2003). These two SCN signaling molecules are capable of phase shifting the circadian clock when administered exogenously. Inactivation of either of these two genes led to mice with altered or arrhythmic behavior in constant darkness, similar to that seen in *Six6*-/- mice. Additionally, *VIP/PHI* knock-out mice under a 1:11 skeleton photoperiod did not display a subjective day and subjective night; this is also similar to the activity patterns observed for the *Six6* knock-out mice. Another similarity that the *Six6*-/- mice share with *VIP/PHI* knock-out mice is an increased number of activity bouts, with increased activity during subjective day in constant darkness. In constant darkness, the ultradian activity patterns of the *Six6*-/- mice lacking optic nerves are qualitatively similar to *VIP/PHI* knock-out mice.

An important difference between the *Six6*-/- and *VIP/PHI* knock-out mice is their response to light-induced behavioral masking. While a mouse with no optic nerves is functionally blind, and thus immune to such masking, the *Six6*-/- mice with one or more intact optic nerves did not display the masking observed for *VIP/PHI* knock-out mice. *Six6*-/- mice increased their wheel running during a discreet one hour light pulse. This abnormal response to light is not likely due to a general failure of the RHT to innervate the SCN, as these *Six6*-/- mice are able to entrain to a normal photoperiod. One fundamental difference from the *VIP/PHI* knock-out mice, however, is the abnormalities seen in the optic nerve and within the SCN itself in the *Six6*-/- mouse.

Whether or not the optic nerves of *Six6*-/- mice form properly during development and then atrophy, or do not form at all, remain interesting questions. While further studies are needed to explore the relationship between optic nerve formation and SCN development, the SCN are not present in any *Six6*-/- mice. This

finding ruled out an obvious hypothesis that the SCN phenotype of the *Six6*-/- mice is secondary to the optic nerve phenotype.

However, *Six6*-/- mice with partially spared optic nerves show some behavioral circadian rhythmicity, while completely lacking SCN. While the role Six6 plays in the molecular clock—if any—is currently unknown, it is possible that *Six6*-/- mice have a functioning cellular circadian clock in the absence of SCN. If the clock is intact in peripheral organs (e.g., the liver), it may function there to preserve some of the behavioral rhythmicity observed in the SCN-lacking *Six6*-/- mice (Figs. 2.3 and 2.5). The *Six6* knock-out mouse therefore serves as an excellent model with which this possibility may be explored.

Material from Chapter 2 has been submitted for publication in the Journal of Biological Rhythms. The author of this dissertation is the first author of this paper. Clark, Daniel D.; Gorman, Michael R.; Mellon, Pamela L. “The Homeodomain Protein Six6 is Required for Development of the Suprachiasmatic Nucleus and Circadian Rhythms.”

Chapter 3: Bmal is Required for Normal Reproductive Behavior and Neuroendocrine Physiology in Mice

Chapter 3.1: Introduction

The mammalian molecular circadian clock is comprised of several interacting transcription/translation feedback loops. One of the most well-characterized of these involves the proteins Clock and Bmal (Arntl1) and the Period (Per) and Cryptochrome (Cry) proteins. Briefly, Clock and Bmal heterodimerize and activate the *Per* and *Cry* genes, which then are translated and translocate back into the nucleus where they inhibit transcriptional activity of Bmal and Clock (Ueda, 2005). Many other genes are involved in related and interconnected transcriptional loops, but the *Bmal* gene has been identified as one of the most crucial elements of the circadian clock. Though a close homologue of *Bmal1* exists in many mammals [*Bmal2*, *Arntl2, (Shi, 2010)*], its presence is apparently not sufficient to compensate for loss of *Bmal1*: knock-out of *Bmal1* effectively stops the circadian clock (Bunger, 2000).

The *Bmal* knock-out mouse has profound phenotypes including those related to the circadian clock. This mouse was originally created via homologous recombination-mediated deletion of the bHLH domain-containing exon of the *Bmal* gene (Bunger, 2000). The *Bmal* knock-out mouse showed no behavioral circadian rhythmicity in the absence of external environmental cues (e.g. photoperiod). However, additional phenotypes were subsequently identified, including lower body weight, tendon calcification, early senescence, and impaired fertility (Bunger, 2000; Kondratov, 2006).

The fertility phenotype of the *Bmal* knock-out mouse has been reported on by several labs. Female *Bmal*-/- mice are infertile, having lengthened or variable estrous

cycles (Boden, 2010), significantly reduced serum progesterone concentrations, and a progesterone-dependent failure of embryos to implant in the uterus (Ratajczak, 2009). Male *Bmal*-/- mice are infertile and have altered steroidogenesis and significantly impaired gonadal function including lower testes weight, reduced sperm count, and smaller seminiferous tubule and seminal vesicle sizes (Alvarez, 2008).

Several important questions regarding *Bmal*-/- mouse reproductive physiology and behavior remain unaddressed. One key physiological role the circadian system is known to play in female rodent reproduction is the gating of the LH surge to a specific window of circadian time (Bronson, 1979). The timing of the LH surge has not yet been addressed in the *Bmal*-/- mouse. Additionally, only anecdotal evidence (Alvarez, 2008) exists regarding the sexual behavior of male mice. With significant but small impairments in gonadal function, it remains unclear whether male *Bmal*-/- mice have impairments in sexual behavior or physiological function or both. We addressed these key questions of *Bmal*-/- mouse reproductive behavior and physiology.

Because the circadian clock is known to play several roles in reproductive biology, and because inactivation of *Bmal* causes infertility along with circadian phenotypes, several approaches were taken to investigate the role *Bmal* plays in fertility. A transgenic approach was used to determine whether tissue-specific inactivation of *Bmal* in all neurons, or in only GnRH neurons, leads to any fertility defects. Serum hormone levels were measured in female *Bmal*-/- mice following ovariectomy and estrogen treatment, to determine whether neuroendocrine physiology was impaired in these mice. Finally, behavioral analysis of *Bmal*-/- mice was carried out to determine if mating behavior was normal in the male KO mice.

Chapter 3.2: Materials and Methods

Creation of transgenic mice. *Bmal*-flox mice (strain B6.129S4(Cg)-Arntl^{tm1Weit}/J) were obtained from Jackson Laboratories (Bar Harbor, ME); this line was submitted to the Jackson laboratories after being backcrossed at least 6 generations onto the C57BL/6 background strain (BL/6). *Bmal*-flox mice were bred to 1) Synapsin-cre mice [as described in (Ma, 1999)] in order to achieve neuron-specific inactivation of *Bmal*, 2) GnRH-cre mice (Yoon, 2005) in order to achieve GnRH neuron-specific inactivation of *Bmal,* or 3) Zp3-cre mice (Lewandoski, 1997) to achieve germline recombination and thus obtain whole-body, germline knock-out animals. The floxed allele (Storch, 2007) deletes the same portion of the gene (most of the basic helix-loop-helix-containing exon 8, as well as exon 9) that is deleted in the *Bmal*-/- mouse reported previously (Bunger, 2000). Each Cre line used was maintained as a continuous backcross to BL/6. Genotyping was performed using tail DNA and the PCR oligonucleotides in Table 3.1. All animal work was performed in accordance with UCSD Institutional Animal Care and Use Committee-approved protocols. Utmost care was taken to ensure the animals were treated humanely and did not suffer.

Table 3.1. Sequences of genotyping oligonucleotides. DNA primers used to genotype mice of the various strains. Multiplex PCR with the three listed *Bmal* ("BMF") primers allowed for genotyping the wild-type, floxed and knock-out alleles.

Primer	Sequence 5' to 3'
Cre_Forward	GCATTACCGGTCGTAGCAACGAGTG
Cre_Reverse	GAACGCTAGAGCCTGTTTTGCACGTTC
BMF.L1_Forward	ACTGGAAGTAACTTTATCAAACTG
BMF.R4_Forward	CTCCTAACTTGGTTTTTGTCTGT
BMF.L2_Reverse	CTGACCAACTTGCTAACAATTA

Pubertal onset. Female pubertal onset was measured by observation of the day of vaginal opening. At weaning, female mice were monitored daily for vaginal opening. Male mice were monitored daily for preputial separation as described previously for rats (Korenbrot, 1977). Day of preputial separation was recorded for full preputial separation only; partial separation was not scored, as all mice showed a similar range of days from partial to full preputial separation. Animal weights were recorded following each daily pubertal onset check.

Ovariectomy and ovarian transplant. *Bmal*-/- and WT mice were anesthetized and ovaries were exposed via a small cut in the skin and peritoneal cavity. For ovariectomy, a loop of surgical suture thread was knotted at the base of the oviducts and the oviduct, ovary, and ovarian fat pad were removed. For ovarian transplant, a tiny cut in the bursa was carefully made using microdissection tools, and the ovary was removed, halved with surgical scissors, and placed briefly into a sterile 0.9% saline solution. An ovary half of the opposite genotype mouse (e.g. WT ovary into KO mouse, or KO ovary into WT mouse) was then carefully reintroduced to the bursa, and the bursa was carefully enclosed around the donor ovary until the bursa self-

adhered. The transplanted ovary, uterine horn, and ovarian fat pad were then reintroduced into the peritoneal cavity, which was sutured closed (Chromic Gut Suture Info). The procedure (ovariectomy or transplant) was repeated bilaterally, as indicated in the Results section (Chapter 3.3). The skin was closed using surgical wound clips. To ensure a healthy and pain-free recovery, mice were given an immediate subcutaneous dose of Buprenorphine anesthetic (Buprenex, 1.2 mg/kg), were allowed to recover overnight, and were given a second dose the following morning. Anesthetic beyond these two doses was not required, as daily health monitoring of post-surgical mice revealed no obvious signs of discomfort (e.g. lack of grooming or feeding, lethargy, etc.).

Hormonal induction of the LH surge. Female *Bmal*-/- and WT mice were ovariectomized and implanted with silastic tubing- and silastic adhesive- (0.04" ID, 0.085" OD; Dow Corning Corp.; Midland, MI) encapsulated estradiol benzoate (EB, 2.5 µg EB per 1 cm capsule). Between ZT3 and ZT4 on day 5 following ovariectomy, female mice were injected with 0.5 µg/0.5 ml estradiol in sesame oil. At ZT12 on day 6 following ovariectomy, and again at ZT2 on day 7, 100 µl blood samples were taken via the tail, and serum was isolated. The LH radioimmunoassay (RIA) was conducted by the University of Virginia Core Ligand and Assay Laboratory.

Plug check behavioral assay. Two to four month old male *Bmal*-/- and WT littermates were each paired with a single WT female eight to twelve weeks of age. At approximately ZT2 each day following introduction of the female into the male's cage, the female was checked for the presence of a vaginal copulatory plug. The female was removed from the male's cage following successful mating; all plugged females

were monitored for pregnancy, and all plugged females became pregnant. Monitoring was continued for a maximum of ten days for each male.

Male sex behavior assessment. Female “stimulator” females were prepared by ovariectomizing WT female mice 8-10 weeks of age. Stimulator females each received silastic-encapsulated estradiol benzoate (see above). At ZT3.5 on day 0 of a trial mating, each stimulator female received a 1 µg subcutaneous dose of estradiol in sesame oil. At ZT8 on day 1 of a trial mating, each stimulator female received a 500 µg dose of progesterone in sesame oil. Each stimulator female was given three trial matings with a male mouse with previous successful breeding experience—each trial was separated by at least five days. Following the three trial matings, *Bmal*-/- and WT male experimental mice were introduced to the stimulator females for two trial matings separated by at least four days. The third mating between the experimental male mice and the stimulator female mice was scored for sex behavior.

Orchidectomy. Male *Bmal*-/- and WT mice were anesthetized and the testes were exposed following small incisions in the scrotal skin and underlying body wall. Small loops of absorbable suture were knotted securely at the base of each testis, and the testis was removed. Sutures were used to close the surgical incisions. Each male received a subcutaneous implant of testosterone as previously described (Kauffman, 2007; Scordalakes, 2003): 1 cm of silastic tubing was packed with crystalline testosterone and sealed with silastic adhesive. T capsules were implanted subcutaneously under the skin of the back during the time of orchidectomy.

Chapter 3.3: Results

Circadian behavioral phenotype of neuron-specific Bmal-/- mice. *Bmal*-/- mice and *Bmal*-floxed mice positive or negative for Syn-cre were subjected to various photoperiod manipulations, and their wheel running activity was measured (Fig. 3.1). During the standard 12:12 photoperiod, wild-type and conditional *Bmal*-/- mice entrained normally and showed consolidated activity bouts during the dark portions of the photoperiod. *Bmal*-/- mice showed an overall decrease in activity. Upon release into constant darkness (with dim illumination as described in the Materials and Methods section), B*mal*-/- mice had arrhythmic, dampened wheel running patterns. Wild-type mice displayed a characteristic <24-hour period of rhythmicity with a stark activity onset ($\tau = 23.8 \pm 0.2$, $n = 9$). Neuron-specific *Bmal*-/- mice also showed robust circadian rhythmicity when released into constant darkness, but with a significantly shorter period ($p < 0.005$, $\tau = 23.3 \pm 0.2$, $n = 6$). Under alternative photoperiods, Cre+ and Cre- mice entrained to the light:dark cycle quickly and robustly, while the KO animals continued to show arrhythmic wheel-running behavior with slightly increased activity during the dark portion of the photoperiod.

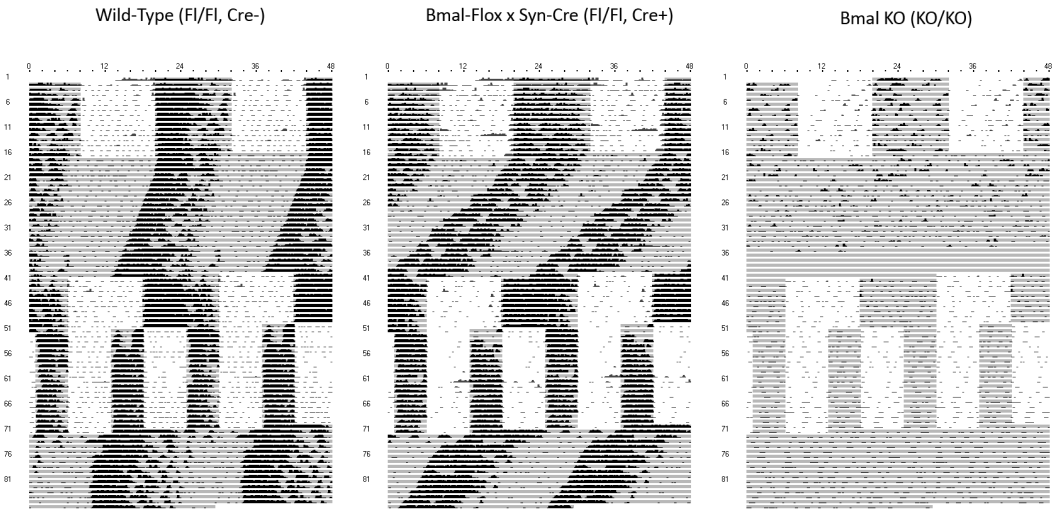

Figure 3.1. Circadian phenotype of neuron-specific Bmal-/- mice. Actograms representative of the wheel-running activity of the three genotypes shown. Five photoperiod manipulations were performed for one to three weeks each (light gray background indicates the dark portion of these photoperiods): 12:12 L:D, constant darkness, 12:12, 6:6:6:6 L:D:L:D, and constant darkness.

There are several possible reasons for the fact that no striking circadian phenotype was observed in the Cre+ animals. Animals bearing the floxed allele of *Bmal* and the *Synapsin*-cre transgene may not have complete targeted recombination (inactivation of *Bmal*) in all central neurons. Other cell types in the brain would have intact *Bmal* and may signal directly or via metabolic status to neurons with a presumably inoperative molecular clock. The brain may be receiving input from peripheral organs such as the liver, signaling to and entraining the animal's behavior in the place of an inactivated clock.

Normal reproductive phenotype of neuron-specific *Bmal* knock-out mice. Pubertal onset in the *Bmal*-flox mice either positive for (n = 6, age at V.O. = 24.0±0.5 d) or negative for (n = 4, age at V.O. = 22.8±0.6 d) the Syn-cre transgene was not statistically different ($p > 0.16$, Student's t-test). Additionally, WT female mice positive

for the Syn-cre transgene were routinely used as colony breeders, and no differences in time to first litter, time between litters, or litter size were observed relative to female mice negative for the Cre transgene.

Normal fertility of female GnRH neuron-specific *Bmal* knock-out mice. Four *Bmal*-flox, GnRH-cre positive and four *Bmal*-flox, GnRH-cre negative littermates were paired with 8-12 week old wild type male mice, and the number of pups and days of birth recorded. No significant differences were found between the two groups in the number of pups per litter, the time until first litter, the time between litters, or any other gross measure of fertility (Fig. 3.2).

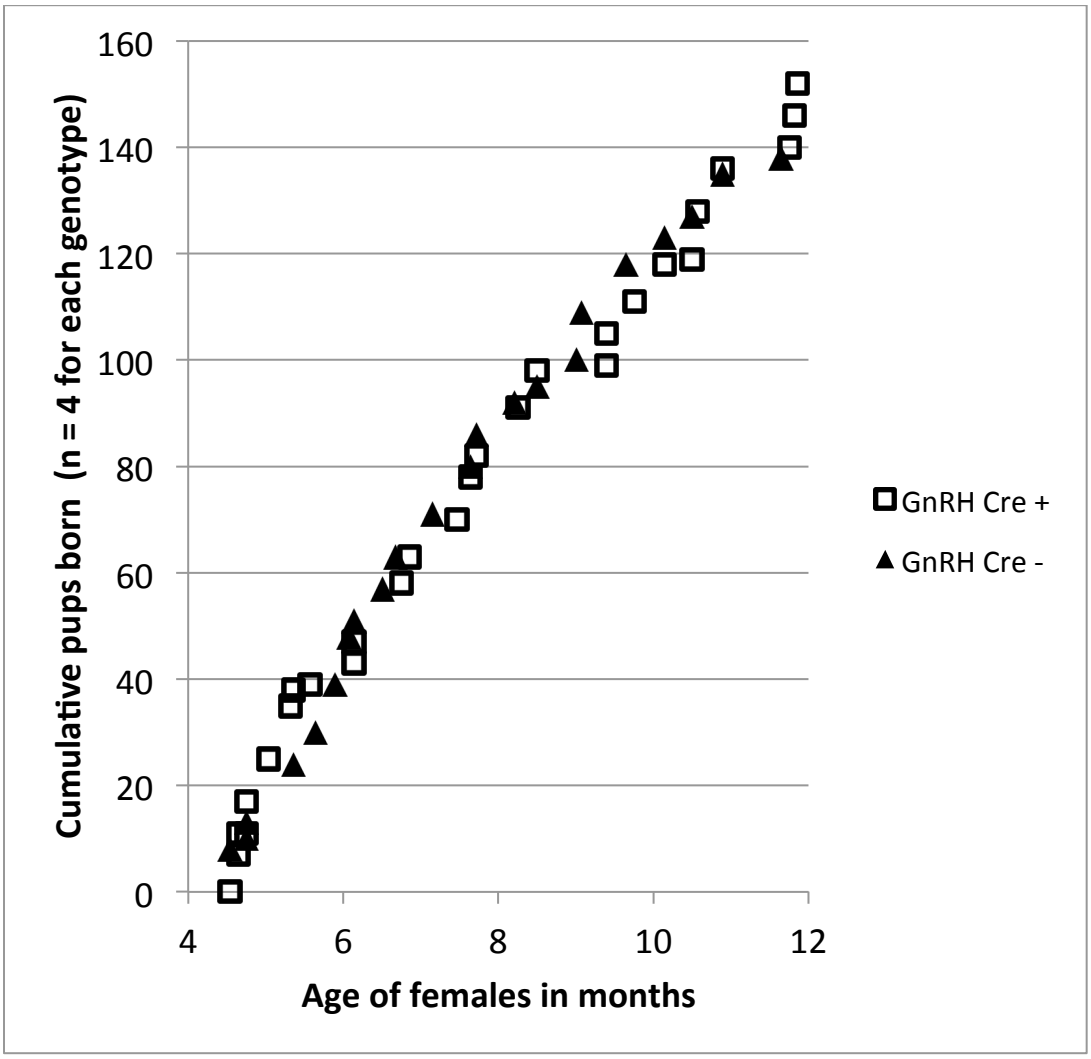

Figure 3.2. Normal fertility of female neuron-specific Bmal knock-out mice. Four GnRH-cre positive and four GnRH-cre negative female Bmal-flox mice fertility assessment. No differences were seen in the cumulative number of pups born to females of the two genotypic groups.

Pubertal onset of the germ-line null *Bmal*-/- mice. Due to the lack of any strong reproductive phenotype in the floxed Bmal x Syn-Cre neuron-specific null mice, we turned to studying the germline, complete null *Bmal*-/- mouse phenotypes. Vaginal opening in female *Bmal*-/- mice was not significantly advanced or delayed relative to

wild-type females ($p > 0.3$, one way ANOVA). WT females showed vaginal opening at 29.9±1.9 days of age (n = 7); HET females showed vaginal opening at 31.5±2.5 days of age (n = 4); and KO females showed vaginal opening at 26.7±2.01 days of age (n = 6; Fig. 3.3). Weights at time of vaginal opening did not significantly differ between the genotypes: WT (n = 5): 14.9±0.6 g, HET (n = 4): 14.4±0.7 g, KO (n = 3): 16.1±0.8 g.

Pubertal onset in male *Bmal*-/- mice was assessed by noting the age at which full preputial separation occurred (Fig 3.3). Age (in days) at preputial separation was 30.1±1.7 for WT (n = 9), 31.1±1.7 for HET (n = 9), and 37.0±1.8 for KO (n = 8). This was significantly higher in KO males than in HET or WT males (one-way ANOVA, $p < 0.05$, Student's t-test). However, animal weights were recorded for males of each genotype at their day of preputial separation. WT mice (n = 4) weighed 14.6±0.7 g, HET mice (n = 9) weighed 15.1±0.5 g, and KO mice weighed 17.0±0.8 g. There was no significant difference in weight at preputial separation between the three groups (one-way ANOVA, $p = 0.08$). This indicates that the age of pubertal onset is secondary to the low body weight phenotype of the *Bmal*-/- mouse, which is observed in males perhaps due to WT males gaining weight faster than female littermates.

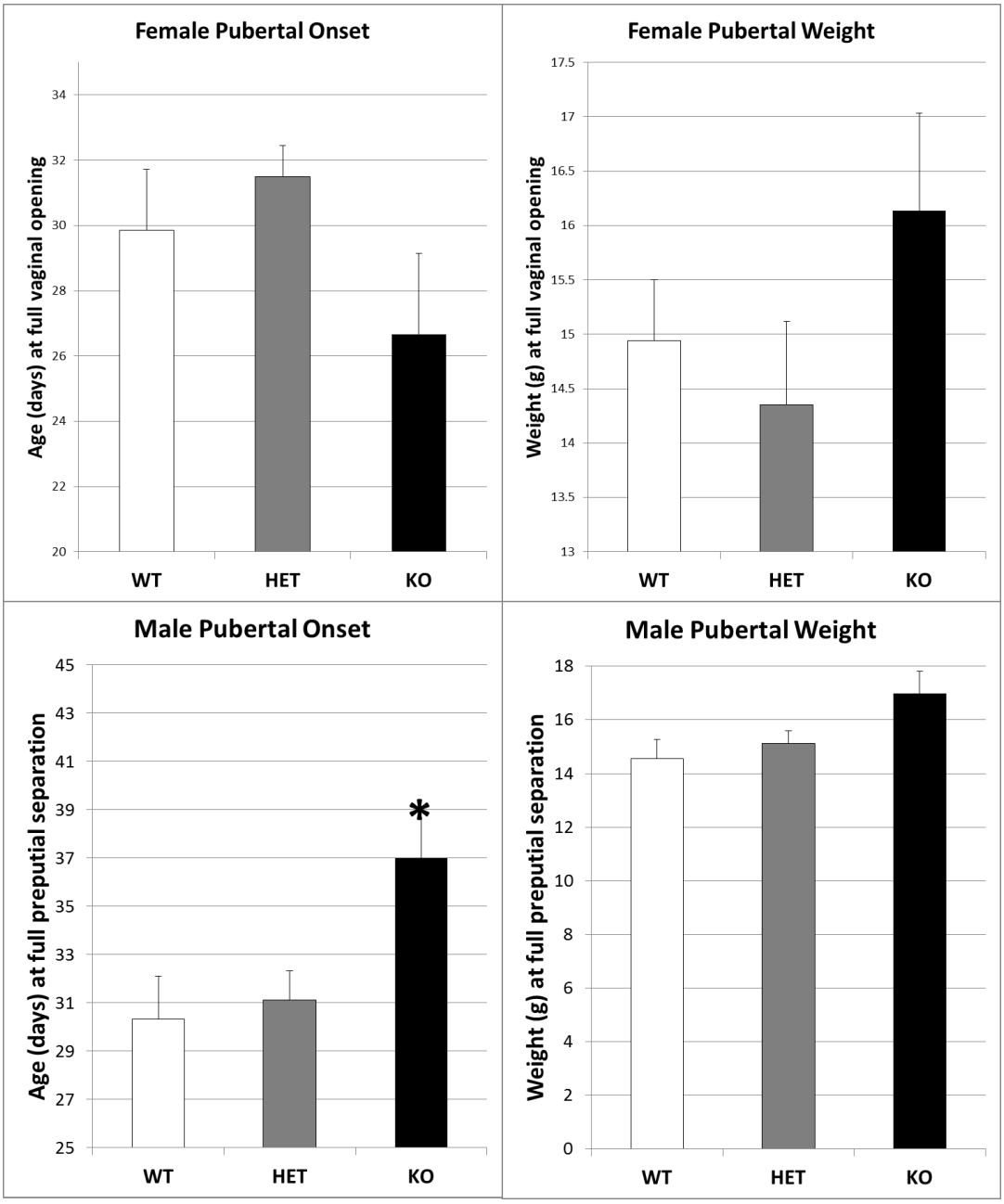

Figure 3.3. Pubertal onset of Bmal-/- mice. Age at vaginal opening or preputial separation is shown in the left two charts. Weight at day of pubertal onset measure shown for the three genotypes in each gender. See text for number of mice in each group and statistical tests performed.

Male *Bmal*-/- mice hormone levels. Male KO and WT littermates were assessed for serum LH, FSH, and testosterone levels (Fig. 3.4). None of these three hormones showed statistically significant differences between the three genotype groups. LH concentrations between the three groups (WT, n = 11; HET, n = 12; KO, n = 11) had one-way ANOVA p-value of 0.33, FSH concentrations (WT, n = 12; HET, n = 12; KO, n = 11) had a p-value of 0.27, and testosterone concentrations (WT, n = 12; HET, n = 12; KO, n = 11) had a p-value of 0.814. These results were surprising, given previous reports on the serum hormone levels of *Bmal*-/- mice (Alvarez, 2008).

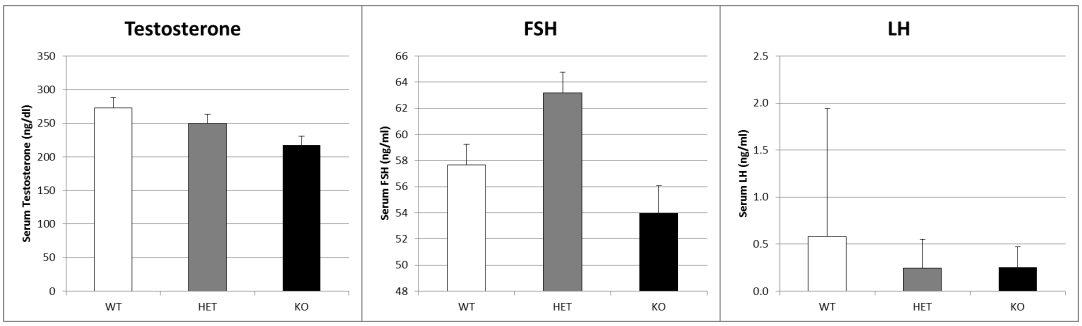

Figure 3.4. Male serum hormone concentrations. Wild-type, heterozygous, and knock-out *Bmal* animals' serum levels of Testosterone, FSH, and LH.

Inability of *Bmal*-/- male mice to plug female mice. WT (n = 4), HET (n = 3), and KO (n = 4) male mice age 2-4 months were housed individually for one week. WT female mice age 8-12 weeks were then introduced into each male's cage and were daily checked for copulatory plugs. WT and HET males were able to plug female mice, with all males successfully forming copulatory plugs with female mates within 5

days (Fig. 3.5). However, *Bmal*-/- mice were unable to form plugs with female mates even after 10 days of continuous mating.

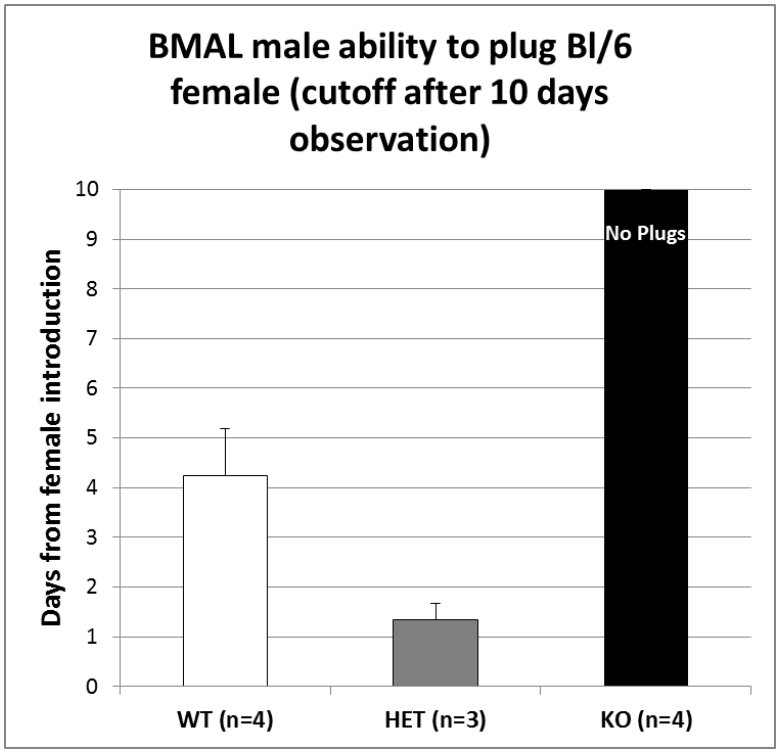

Figure 3.5. *Bmal*-/- ability to plug females. Male *Bmal*-/- and WT animals' ability to plug WT female mice. No *Bmal*-/- mouse formed a copulatory plug within the period of daily observation, while HET and WT mice were all able to do so.

Impaired sexual behavior of *Bmal*-/- male mice. Sexually receptive stimulator female mice were prepared as described in the Materials and Methods section. Male WT (n = 4) and KO (n = 4) mice were given two rounds of mating experience with one stimulator female each prior to assessing behavior. On the third mating trial, sexual behavior was scored for 30 minutes following introduction of the stimulator female to

each male's cage. The number of mounting attempts, and number of seconds spent mounting during the period of observation is given in Figure 3.6. No *Bmal*-/- male mouse attempted any mounting of the sexually receptive female mate.

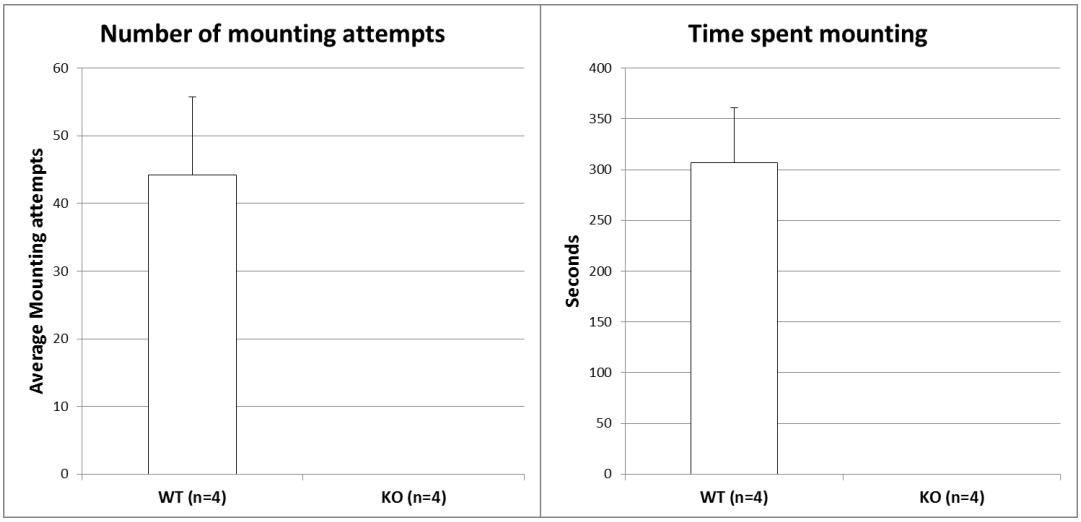

Figure 3.6. *Bmal*-/- sex behavior. Male *Bmal*-/- mice do not show normal sex behaviors, while WT littermates do, during the 30 minute period of observation.

Impaired sexual behavior in T-implanted *Bmal*-/- male mice. Because male mating behavior heavily relies on serum testosterone levels (Luttge, 1973), the sexual behavior assessment was repeated for WT (n = 3) and KO (n = 3) mice that had been castrated and given testosterone implants, as described in the Materials and Methods section. After the requisite stimulator female preparation and two-trial experience matings, sexual behavior in the castrated, testosterone-implanted mice were scored for 30 minutes following introduction of a sexually receptive female into the cage. Again, WT mice showed numerous mounting attempts, and spent several minutes of

the observation period in the mounting position (Fig. 3.7). However, no *Bmal*-/- mouse attempted to mount the female during the entire period of observation.

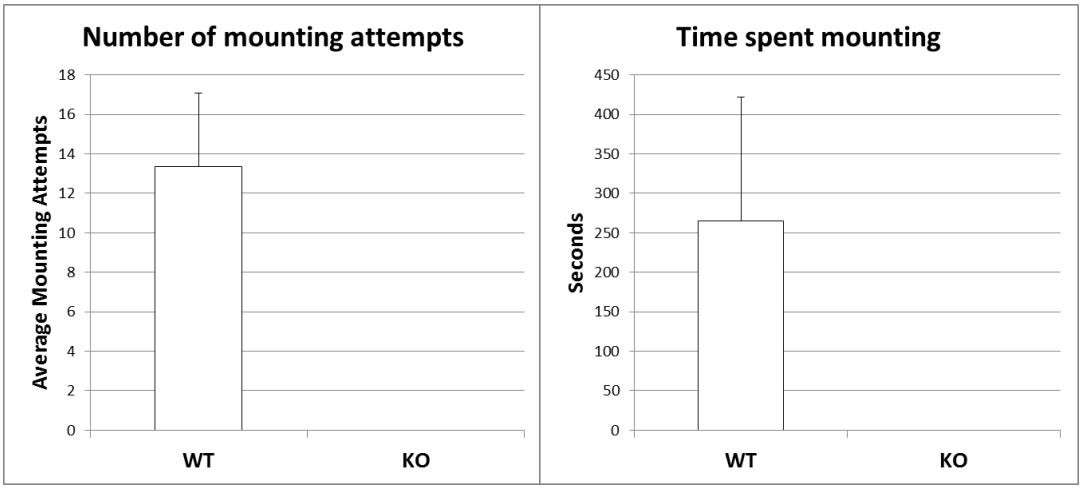

Figure 3.7. *Bmal*-/- sex behavior following T implantation. Sex behavior quantification of wild-type (n = 3) and *Bmal*-/- mice (n = 3) following castration and T implantation as described in the Materials and Methods section. No *Bmal*-/- mouse attempts mounting during the 30 minute period of observation.

Failure of the LH surge induction in *Bmal*-/- female mice. Ovarian hormones, including estrogen, act at the levels of the pituitary and hypothalamus during the estrous cycle to signal the appropriate time of the LH surge. The LH surge can be experimentally induced *in vivo* by normalizing the estrogen concentration by ovariectomy and estrogen replacement, followed by supplying an exogenous high dose of estrogen (Materials and Methods). Wild-type and *Bmal*-/- female mice were subjected to this LH surge protocol, and serum LH was measured at two time points: the evening of the induced LH surge, when LH levels should be maximal, and the morning following the LH surge induction, when LH levels should have returned to

baseline levels due to the low background estrogen induced by the implant. WT females (n = 5) responded to the surge paradigm with robust LH inductions at the appropriate time, and low LH the following morning (n = 7; Fig. 3.8). KO females, however, did not show an LH surge on the evening of the intended induction (n = 8). LH concentrations remained low in the KO females on the following morning (n = 5).

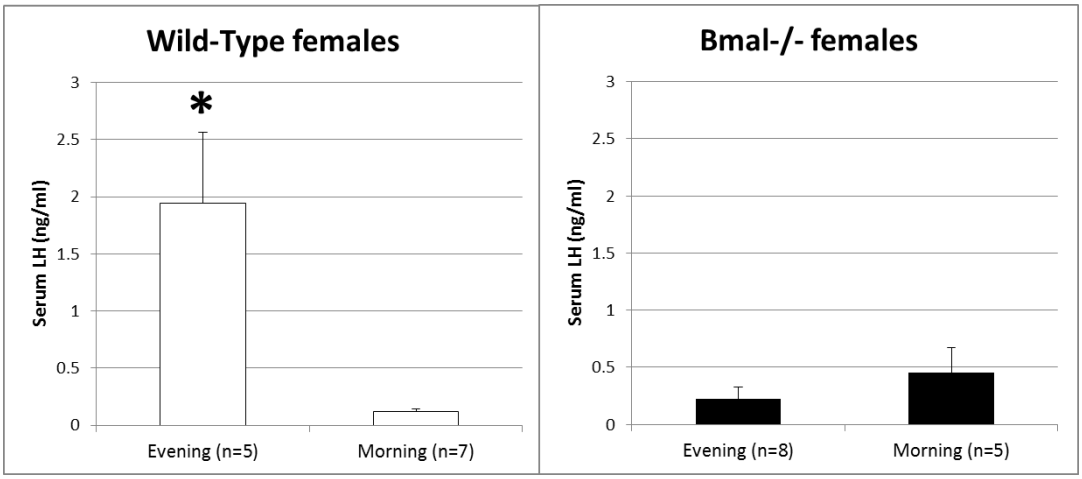

Figure 3.8. *Bmal*-/- female LH surge induction. Serum LH levels of WT and *Bmal*-/- mice following estrogen priming reveals that *Bmal*-/- mice are incapable of mounting an LH surge in response to estrogen.

Chapter 3.4: Discussion

Of the known genes of the circadian clock, only a dominant-negative mutation of *Clock* or inactivation of *Bmal* appears to result in fertility deficits. This is perhaps due to the mild circadian phenotype resultant from many of these genetic manipulations, though inactivation of multiple genes [multiple *Per* or *Cry* gene knock-out mice (Van Der Horst, 1999)] results in a stronger circadian impairment

(arrhythmicity in constant darkness) with only mild reproductive impairments, if any. The female Clock$^{\Delta 19}$ mutant mouse has a striking reproductive phenotype: longer estrous cyclicity, and pregnancy and parturition defects (Chappell, 2003). However, the *Bmal*-/- mouse has the strongest fertility deficit of the circadian mutant/knock-out mice: complete infertility in both sexes.

Some aspects of the HPG axis—primarily the gonads—have been previously investigated in the *Bmal*-/- mouse. The ovaries of these mice are responsive to exogenously administered gonadotropins in a superovulation protocol, and the number of embryos/oocytes released from *Bmal*-/- females following superovulation did not significantly differ from WT females (Ratajczak, 2009). While there is growing evidence for the importance of the circadian clock within the ovary (Sellix, 2010), the ovaries of *Bmal*-/- mice appear to respond normally to gonatotropins. Also, at least some *Bmal*-/- females are able to progress through the estrous cycle (Boden, 2010), indicating that the ovaries progress through their normal pattern of folliculogenesis.

In an attempt to further address the role of *Bmal* in the ovary, ovarian transplants were attempted between WT and KO littermate females between 2-4 months of age, with limited success. Of the WT female recipient mice, most subsequently became pregnant by WT males. However, only three KO/WT pups were born to these females out of several dozen pups—the remaining pups all had WT/WT genotypes. This indicated that the recipient females' ovaries were incompletely removed prior to transplantation of the KO ovary. Thus, *Bmal*-/- mouse ovaries are able to function properly in the context of a WT female recipient. Of the KO females transplanted with wild-type embryos, none subsequently became pregnant.

The testes of *Bmal*-/- mice have minor, but statistically significant functional impairments (Alvarez, 2008): testes weight, sperm count, and seminiferous tubule and seminal vesicle size were each lower in *Bmal*-/- mice, though none of these impairments can explain the complete infertility observed in these males. The observed significant decrease in testosterone concentration reported was not repeatable in the *Bmal*-/- mice in our lab. This discrepancy is not readily accounted for, as the time of blood collection (ZT3), and background strain (C57BL/6 backcross) were identical. However, the original *Bmal*-/- allele previously reported was from a different initial source: the original *Bmal*-/- strain developed by Bunger *et al.* (Bunger, 2000) was different from the germline knock-out produced from the *Bmal*-flox allele (Storch, 2007) in the present studies. Yet, the two knock-out strains used identical approaches for inactivation of the *Bmal* gene: targeted deletion of exon 8, and both lacked circadian rhythms.

Female *Bmal*-/- mice display a lack of an LH surge in response to estrogen. This is in agreement with previous work on the $Clock^{\Delta 19}$ female mouse (Miller, 2004). In both types of female mice, ovarian histology is normal, and the females are able to progress through the estrous cycle normally. In the $Clock^{\Delta 19}$ study, the female mice had intact ovaries and were serially sampled over the course of 16 hours. One review speculated that the lack of an LH surge in the mutant mice but not the wild-type may reflect an increased sensitivity to the frequent handling of the animals (Boden, 2006). Additionally, estradiol administration failed to elicit an LH surge in ovariectomized $Clock^{\Delta 19}$ females (Kennaway, 2005). How is it that in these females, estrous cyclicity can progress and the ovaries show corpora lutea indicative of ovulations, but the LH surge does not occur?

The present results on *Bmal*-/- female mice unable to respond to estradiol with an LH surge raise similar questions. Further work is needed to test possible hypotheses for this. Perhaps non-endocrine mechanisms for ovulation exist—these could include pheromonal, behavioral-social, or pituitary gonadotropin-independent mechanisms. Future work is needed to explain the lack of an LH surge in female *Bmal*-/- mice. The possibility exists that LH surges do occur at abnormal times, but have not been detected. The induction protocol used for these experiments assumes sensitivity to estrogen, but the expression of estrogen receptor in the appropriate brain and pituitary regions has not been measured.

The profound sexual behavior deficit observed in male *Bmal*-/- mice has several possible explanations. The fact that sexual behavior is not rescued in testosterone-rescued *Bmal*-/- mice indicates that the defect seen in intact Bmal-/- mice is more profound than a simple hormone deficiency. The social and pheromonal cues male mice use for appropriate mating behavior rely on appropriate sexual dimorphism of the brain during development. Additional work is needed to determine whether the brains of *Bmal*-/- male mice properly masculinize in response to developmental cues. Alternately, it is not known if the *Bmal*-/- mouse pheromone system—or, indeed, the sense of smell—is functionally intact. Impairments in either of these could also explain the sexual behavioral findings.

Previous work on the *Bmal*-/- mouse fertility impairment did not address behavioral or estrous cycle physiological mechanisms underlying the reproductive deficits. The results reported here—lack of an LH surge in females and lack of sex behavior in males—provide additional insights into the reproductive deficits of the *Bmal*-/- mouse.

References

1. Aijaz S, Allen J, Tregidgo R, van Heyningen V, Hanson I, Clark BJ: **Expression analysis of six3 and six6 in human tissues reveals differences in expression and a novel correlation between the expression of six3 and the genes encoding isocitrate dehyhrogenase and cadherin 18.** *Genomics* (2005) **86**:86-99.

2. Alvarez JD, Hansen A, Ord T, Bebas P, Chappell PE, Giebultowicz JM, Williams C, Moss S, Sehgal A: **The circadian clock protein bmal1 is necessary for fertility and proper testosterone production in mice.** *J Biol Rhythms* (2008) **23**:26-36.

3. Becker KL: *Principles and practice of endocrinology and metabolism.* Lippincott, Philadelphia, PA (1995).

4. Bianco SD, Kaiser UB: **The genetic and molecular basis of idiopathic hypogonadotropic hypogonadism.** *Nat Rev Endocrinol* (2009) **5**:569-576.

5. Boden MJ, Kennaway DJ: **Circadian rhythms and reproduction.** *Reproduction* (2006) **132**:379-392.

6. Boden MJ, Kennaway DJ: **Reproduction in the arrhythmic *bmal1* knockout mouse.** *Reprod Fertil Dev* (2005) **17**:126-126.

7. Boden MJ, Kennaway DJ: **Reproductive consequences of circadian dysfunction: Fertility in the *bmal1* null mouse.** *Reprod Fertil Dev* (2004) **16**:280-280.

8. Boden MJ, Varcoe TJ, Voultsios A, Kennaway DJ: **Reproductive biology of female bmal1 null mice.** *Reproduction* (2010) **139**:1077-1090.

9. Bradshaw BS, Wolfe HG: **Coagulation proteins in the seminal vesicle and coagulating gland of the mouse.** *Biol Reprod* (1977) **16**:292-297.

10. Brodbeck S, Besenbeck B, Englert C: **The transcription factor six2 activates expression of the gdnf gene as well as its own promoter.** *Mech Dev* (2004) **121**:1211-1222.

11. Bronson FH, Vom Saal FS: **Control of the preovulatory release of luteinizing hormone by steroids in the mouse.** *Endocrinology* (1979) **104**:1247-1255.

12. Bunger MK, Wilsbacher LD, Moran SM, Clendenin C, Radcliffe LA, Hogenesch JB, Simon MC, Takahashi JS, Bradfield CA: **Mop3 is an essential component of the master circadian pacemaker in mammals.** *Cell* (2000) **103**:1009-1017.

13. Challet E: **Interactions between light, mealtime and calorie restriction to control daily timing in mammals.** *J Comp Physiol B* (2010) **180**:631-644.

14. Chappell PE, White RS, Mellon PL: **Circadian gene expression regulates pulsatile gonadotropin-releasing hormone (gnrh) secretory patterns in the hypothalamic gnrh-secreting gt1-7 cell line.** *J Neurosci* (2003) **23**:11202-11213.

15. Chase HB, Chase EB: **Studies on an anophthalmic strain of mice i. Embryology of the eye region.** *J Morphology* (1941) **68**:279-301.

16. Cherrington BD, Bailey JS, Diaz AL, Mellon PL: **Neurod1 and mash1 temporally regulate gnrh receptor gene expression in immortalized mouse gonadotrope cells.** *Mol Cell Endocrinol* (2008) **295**:106-114.

17. Clark ME, Mellon PL: **The pou homeodomain transcription factor oct-1 is essential for activity of the gonadotropin-releasing hormone neuron-specific enhancer.** *Mol Cell Biol* (1995) **15**:6169-6177.

18. Clarkson J, d'Anglemont de Tassigny X, Moreno AS, Colledge WH, Herbison AE: **Kisspeptin-gpr54 signaling is essential for preovulatory gonadotropin-releasing hormone neuron activation and the luteinizing hormone surge.** *J Neurosci* (2008) **28**:8691-8697.

19. Colwell CS, Michel S, Itri J, Rodriguez W, Tam J, Lelievre V, Hu Z, Liu X, Waschek JA: **Disrupted circadian rhythms in vip- and phi-deficient mice.** *Am J Physiol Regul Integr Comp Physiol* (2003) **285**:R939-949.

20. Conte I, Morcillo J, Bovolenta P: **Comparative analysis of six 3 and six 6 distribution in the developing and adult mouse brain.** *Dev Dyn* (2005) **234**:718-725.

21. Cowden KD, Simon MC: **The bhlh/pas factor mop3 does not participate in hypoxia responses.** *Biochem Biophys Res Commun* (2002) **290**:1228-1236.

22. Dodd AN, Salathia N, Hall A, Kevei E, Toth R, Nagy F, Hibberd JM, Millar AJ, Webb AA: **Plant circadian clocks increase photosynthesis, growth, survival, and competitive advantage.** *Science* (2005) **309**:630-633.

23. Dolatshad H, Campbell EA, O'Hara L, Maywood ES, Hastings MH, Johnson MH: **Developmental and reproductive performance in circadian mutant mice.** *Hum Reprod* (2006) **21**:68-79.

24. Fang Z, Xiong X, James A, Gordon DF, Wierman ME: **Identification of novel factors that regulate gnrh gene expression and neuronal migration.** *Endocrinology* (1998) **139**:3654-3657.

25. Gamble JA, Karunadasa DK, Pape JR, Skynner MJ, Todman MG, Bicknell RJ, Allen JP, Herbison AE: **Disruption of ephrin signaling associates with disordered axophilic migration of the gonadotropin-releasing hormone neurons.** *J Neurosci* (2005) **25**:3142-3150.

26. Gibson MJ, Wu TJ, Miller GM, Silverman AJ: **What nature's knockout teaches us about gnrh activity: Hypogonadal mice and neuronal grafts.** *Horm Behav* (1997) **31**:212-220.

27. Givens ML, Kurotani R, N. R-H, Miller NLG, Mellon PL: **Phylogenetic footprinting reveals functional upstream regions of the gonadotropin-releasing hormone gene that enhance cell-specific expression.** *Mol Endocrinol* (2004) **18**:2950-2966.

28. Givens ML, Rave-Harel N, Goonewardena VD, Kurotani R, Berdy SE, Swan CH, Rubenstein JL, Robert B, Mellon PL: **Developmental regulation of gonadotropin-releasing hormone gene expression by the msx and dlx homeodomain protein families.** *J Biol Chem* (2005) **280**:19156-19165.

29. Goldman BD: **The circadian timing system and reproduction in mammals.** *Steroids* (1999) **64**:679-685.

30. Hamilton BA, Frankel WN, Kerrebrock AW, Hawkins TL, FitzHugh W, Kusumi K, Russell LB, Mueller KL, van Berkel V, Birren BW, Kruglyak L *et al*: **Disruption of the nuclear hormone receptor roralpha in staggerer mice.** *Nature* (1996) **379**:736-739.

31. Harris SE, Winchester CL, Johnson KJ: **Functional analysis of the homeodomain protein six5.** *Nucleic Acids Res* (2000) **28**:1871-1878.

32. Herbison AE, Porteous R, Pape JR, Mora JM, Hurst PR: **Gonadotropin-releasing hormone (gnrh) neuron requirements for puberty, ovulation and fertility.** *Endocrinology* (2008) **149**:597-604.

33. Hinds JW, Hinds PL: **Early ganglion cell differentiation in the mouse retina: An electron microscopic analysis utilizing serial sections.** *Dev Biol* (1974) **37**:381-416.

34. Hu S, Mamedova A, Hegde RS: **DNA-binding and regulation mechanisms of the six family of retinal determination proteins.** *Biochemistry* (2008) **47**:3586-3594.

35. Iyer AK, Miller NL, Yip K, Tran BH, Mellon PL: **Enhancers of gnrh transcription embedded in an upstream gene use homeodomain proteins to specify hypothalamic expression.** *Mol Endocrinol* (2010) **24**:1949-1964.

36. Jean D, Bernier G, Gruss P: **Six6 (optx2) is a novel murine six3-related homeobox gene that demarcates the presumptive pituitary/hypothalamic axis and the ventral optic stalk.** *Mech Dev* (1999) **84**:31-40.

37. Kabrita CS, Davis FC: **Development of the mouse suprachiasmatic nucleus: Determination of time of cell origin and spatial arrangements within the nucleus.** *Brain Res* (2008) **1195**:20-27.

38. Kauffman AS, Park JH, McPhie-Lalmansingh AA, Gottsch ML, Bodo C, Hohmann JG, Pavlova MN, Rohde AD, Clifton DK, Steiner RA, Rissman EF: **The kisspeptin receptor gpr54 is required for sexual differentiation of the brain and behavior.** *J Neurosci* (2007) **27**:8826-8835.

39. Kawakami K, Sato S, Ozaki H, Ikeda K: **Six family genes--structure and function as transcription factors and their roles in development.** *Bioessays* (2000) **22**:616-626.

40. Kelley CG, Givens ML, Rave-Harel N, Nelson SB, Anderson S, Mellon PL: **Neuron-restricted expression of the rat gonadotropin-releasing hormone gene is conferred by a cell-specific protein complex that binds repeated caatt elements.** *Mol Endocrinol* (2002) **16**:2413-2425.

41. Kelley CG, Lavorgna G, Clark ME, Boncinelli E, Mellon PL: **The otx2 homeoprotein regulates expression from the gonadotropin-releasing hormone proximal promoter.** *Mol Endocrinol* (2000) **14**:1246-1256.

42. Kennaway DJ: **The role of circadian rhythmicity in reproduction.** *Hum Reprod Update* (2005) **11**:91-101.

43. Kim HH, Wolfe A, Cohen RN, Eames SC, Johnson AL, Wieland CN, Radovick S: **In vivo identification of a 107 bp promoter element mediating neuron-specific expression of mouse gnrh.** *Mol Endocrinol* (2007) **21**:457-471.

44. Kim HH, Wolfe A, Smith GR, Tobet SA, Radovick S: **Promoter sequences targeting tissue-specific gene expression of hypothalamic and ovarian gonadotropin-releasing hormone in vivo.** *J Biol Chem* (2002) **277**:5194-5202.

45. Kondratov RV, Kondratova AA, Gorbacheva VY, Vykhovanets OV, Antoch MP: **Early aging and age-related pathologies in mice deficient in bmal1, the core componentof the circadian clock.** *Genes Dev* (2006) **20**:1868-1873.

46. Korenbrot CC, Huhtaniemi IT, Weiner RI: **Preputial separation as an external sign of pubertal development in the male rat.** *Biol Reprod* (1977) **17**:298-303.

47. Kramer PR, Krishnamurthy R, Mitchell PJ, Wray S: **Transcription factor activator protein-2 is required for continued luteinizing hormone-releasing hormone expression in the forebrain of developing mice.** *Endocrinology* (2000) **141**:1823-1838.

48. Kruger M, Ruschke K, Braun T: **Nscl-1 and nscl-2 synergistically determine the fate of gnrh-1 neurons and control necdin gene expression.** *EMBO J* (2004) **23**:4353-6443.

49. Kumar JP: **The sine oculis homeobox (six) family of transcription factors as regulators of development and disease.** *Cell Mol Life Sci* (2009) **66**:565-583.

50. Laclef C, Hamard G, Demignon J, Souil E, Houbron C, Maire P: **Altered myogenesis in six1-deficient mice.** *Development* (2003) **130**:2239-2252.

51. Laemle LK, Hori N, Strominger NL, Tan Y, Carpenter DO: **Physiological and anatomical properties of the suprachiasmatic nucleus of an anophthalmic mouse.** *Brain Res* (2002) **953**:73-81.

52. Laemle LK, Ottenweller JE: **Daily patterns of running wheel activity in male anophthalmic mice.** *Physiol Behav* (1998) **64**:165-171.

53. Lagutin OV, Zhu CC, Kobayashi D, Topczewski J, Shimamura K, Puelles L, Russell HR, McKinnon PJ, Solnica-Krezel L, Oliver G: **Six3 repression of wnt signaling in the anterior neuroectoderm is essential for vertebrate forebrain development.** *Genes Dev* (2003) **17**:368-379.

54. Larder R, Chang L, Clinton M, Brown P: **Gonadotropin-releasing hormone regulates expression of the DNA damage repair gene, fanconi anemia a, in pituitary gonadotroph cells.** *Biol Reprod* (2004) **71**:828-836.

55. Larder R, Clark DD, Miller NL, Mellon PL: **Hypothalamic dysregulation and infertility in mice lacking the homeodomain protein six6.** *J Neurosci* (2011) **31**:426-438.

56. Larder R, Mellon PL: **Otx2 induction of the gonadotropin-releasing hormone promoter is modulated by direct interactions with grg co-repressors.** *J Biol Chem* (2009) **284**:16966-16978.

57. Lawson MA, Buhain AR, Jovenal JC, Mellon PL: **Multiple factors interacting at the gata sites of the gonadotropin-releasing hormone neuron-specific enhancer regulate gene expression.** *Mol Endocrinol* (1998) **12**:364-377.

58. Lawson MA, MacConell LA, Kim J, Powl BT, Nelson SB, Mellon PL: **Neuron-specific expression in vivo by defined transcription regulatory elements of the gonadotropin-releasing hormone gene.** *Endocrinology* (2002) **143**:1404-1412.

59. Lawson MA, Whyte DB, Mellon PL: **Gata factors are essential for activity of the neuron-specific enhancer of the gonadotropin-releasing hormone gene.** *Mol Cell Biol* (1996) **16**:3596-3605.

60. Leak RK, Moore RY: **Topographic organization of suprachiasmatic nucleus projection neurons.** *J Comp Neurol* (2001) **433**:312-334.

61. Lewandoski M, Wassarman KM, Martin GR: **Zp3-cre, a transgenic mouse line for the activation or inactivation of loxp-flanked target genes specifically in the female germ line.** *Curr Biol* (1997) **7**:148-151.

62. Li X, Perissi V, Liu F, Rose DW, Rosenfeld MG: **Tissue-specific regulation of retinal and pituitary precursor cell proliferation.** *Science* (2002) **297**:1180-1183.

63. Lincoln GA, Almeida OF, Arendt J: **Role of melatonin and circadian rhythms in seasonal reproduction in rams.** *J Reprod Fertil Suppl* (1981) **30**:23-31.

64. Liu W, Lagutin OV, Mende M, Streit A, Oliver G: **Six3 activation of pax6 expression is essential for mammalian lens induction and specification.** *EMBO J* (2006) **25**:5383-5395.

65. Lopez-Rios J, Gallardo ME, Rodriguez de Cordoba S, Bovolenta P: **Six9 (optx2), a new member of the six gene family of transcription factors, is expressed at early stages of vertebrate ocular and pituitary development.** *Mech Dev* (1999) **83**:155-159.

66. Lund RD, Blunt AH: **Prenatal development of central optic pathways in albino rats.** *J Comp Neurol* (1976) **165**:247-264.

67. Luttge WG, Hall NR: **Differential effectiveness of testosterone and its metabolites in the induction of male sexual behavior in two strains of albino mice.** *Hormones and Behavior* (1973) **4**:31-43.

68. Ma L, Reis G, Parada LF, Schuman EM: **Neuronal nt-3 is not required for synaptic transmission or long-term potentiation in area ca1 of the adult rat hippocampus.** *Learn Mem* (1999) **6**:267-275.

69. Mason CA, Sparrow N, Lincoln DW: **Structural features of the retinohypothalamic projection in the rat during normal development.** *Brain Res* (1977) **132**:141-148.

70. McGillivray SM, Bailey JS, Ramezani R, Kirkwood BJ, Mellon PL: **Mouse gnrh receptor gene expression is mediated by the lhx3 homeodomain protein.** *Endocrinology* (2005) **146**:2180-2185.

71. Mellon PL, Windle JJ, Goldsmith P, Padula C, Roberts J, Weiner RI: **Immortalization of hypothalamic gnrh neurons by genetically targeted tumorigenesis.** *Neuron* (1990) **5**:1-10.

72. Miller BH, Olson SL, Turek FW, Levine JE, Horton TH, Takahashi JS: **Circadian clock mutation disrupts estrous cyclicity and maintenance of pregnancy.** *Curr Biol* (2004) **14**:1367-1373.

73. Miller NL, Wevrick R, Mellon PL: **Necdin, a prader-willi syndrome candidate gene, regulates gonadotropin-releasing hormone neurons during development.** *Hum Mol Genet* (2009) **18**:248-260.

74. Nagai N, Nagai K, Nakagawa H: **Effect of orbital enucleation on glucose homeostasis and morphology of the suprachiasmatic nucleus.** *Brain Res* (1992) **589**:243-252.

75. Nelson SB, Lawson MA, Kelley CG, Mellon PL: **Neuron-specific expression of the rat gonadotropin-releasing hormone gene is conferred by interactions of a defined promoter element with the enhancer in gt1-7 cells.** *Mol Endocrinol* (2000) **14**:1509-1522.

76. Niinuma K, Someya N, Kimura M, Yamaguchi I, Hamamoto H: **Circadian rhythm of circumnutation in inflorescence stems of arabidopsis.** *Plant Cell Physiol* (2005) **46**:1423-1427.

77. Oliver G, Mailhos A, Wehr R, Copeland NG, Jenkins NA, Gruss P: **Six3, a murine homologue of the sine oculis gene, demarcates the most anterior border of the developing neural plate and is expressed during eye development.** *Development* (1995) **121**:4045-4055.

78. Ozaki H, Nakamura K, Funahashi J, Ikeda K, Yamada G, Tokano H, Okamura HO, Kitamura K, Muto S, Kotaki H, Sudo K *et al*: **Six1 controls patterning of the mouse otic vesicle.** *Development* (2004) **131**:551-562.

79. Panda S, Provencio I, Tu DC, Pires SS, Rollag MD, Castrucci AM, Pletcher MT, Sato TK, Wiltshire T, Andahazy M, Kay SA *et al*: **Melanopsin is required for non-image-forming photic responses in blind mice.** *Science* (2003) **301**:525-527.

80. Panda S, Sato TK, Castrucci AM, Rollag MD, DeGrip WJ, Hogenesch JB, Provencio I, Kay SA: **Melanopsin (opn4) requirement for normal light-induced circadian phase shifting.** *Science* (2002) **298**:2213-2216.

81. Pierce A, Bliesner B, Xu M, Nielsen-Preiss S, Lemke G, Tobet S, Wierman ME: **Axl and tyro3 modulate female reproduction by influencing gonadotropin-releasing hormone neuron survival and migration.** *Mol Endocrinol* (2008) **22**:2481-2495.

82. Pitteloud N, Quinton R, Pearce S, Raivio T, Acierno J, Dwyer A, Plummer L, Hughes V, Seminara S, Cheng YZ, Li WP *et al*: **Digenic mutations account for variable phenotypes in idiopathic hypogonadotropic hypogonadism.** *J Clin Invest* (2007) **117**:457-463.

83. Pittendrigh CS, Daan S: **A functional analysis of circadian pacemakers in nocturnal rodents. Iv: Entrainment: Pacemaker as clock.** *J Comp Physiol A* (1976) **106**:291-331.

84. Radovick S, Wray S, Lee E, Nicols DK, Nakayama Y, Weintraub BD, Westphal H, Cutler J, G B, Wondisford FE: **Migratory arrest of gonadotropin-releasing hormone neurons in transgenic mice.** *Proc Natl Acad Sci USA* (1991) **88**:3402-3406.

85. Ratajczak CK, Boehle KL, Muglia LJ: **Impaired steroidogenesis and implantation failure in bmal1-/- mice.** *Endocrinology* (2009) **150**:1879-1885.

86. Rave-Harel N, Givens ML, Nelson SB, Duong HA, Coss D, Clark ME, Hall SB, Kamps MP, Mellon PL: **Tale homeodomain proteins regulate gonadotropin-releasing hormone gene expression independently and via interactions with oct-1.** *J Biol Chem* (2004) **279**:30287-30297.

87. Rave-Harel N, Miller NL, Givens ML, Mellon PL: **The groucho-related gene family regulates the gonadotropin-releasing hormone gene through interaction with the homeodomain proteins msx1 and oct1.** *J Biol Chem* (2005) **280**:30975-30983.

88. Schwanzel-Fukuda M, Abraham S, Crossin KL, Edelman GM, Pfaff DW: **Immunocytochemical demonstration of neural cell adhesion molecule (ncam) along the migration route of luteinizing hormone-releasing hormone (lhrh) neurons in mice.** *J Comp Neurol* (1992) **321**:1-18.

89. Schwanzel-Fukuda M, Pfaff DW: **Origin of luteinizing hormone-releasing hormone neurons.** *Nature* (1989) **338**:161-164.

90. Scordalakes EM, Rissman EF: **Aggression in male mice lacking functional estrogen receptor alpha.** *Behav Neurosci* (2003) **117**:38-45.

91. Sellix MT, Menaker M: **Circadian clocks in the ovary.** *Trends Endocrinol Metab* (2010) **21**:628-636.

92. Seo HC, Curtiss J, Mlodzik M, Fjose A: **Six class homeobox genes in drosophila belong to three distinct families and are involved in head development.** *Mech Dev* (1999) **83**:127-139.

93. Shi S, Hida A, McGuinness OP, Wasserman DH, Yamazaki S, Johnson CH: **Circadian clock gene bmal1 is not essential; functional replacement with its paralog, bmal2.** *Curr Biol* (2010) **20**:316-321.

94. Shima H, Tsuji M, Young P, Cunha GR: **Postnatal growth of mouse seminal vesicle is dependent on 5 alpha-dihydrotestosterone.** *Endocrinology* (1990) **127**:3222-3233.

95. Silver J: **Abnormal development of the suprachiasmatic nuclei of the hypothalamus in a strain of genetically anophthalmic mice.** *J Comp Neurol* (1977) **176**:589-606.

96. Simerly RB, Swanson LW, Gorski RA: **The distribution of monoaminergic cells and fibers in a periventricular preoptic nucleus involved in the control of gonadotropin release: Immunohistochemical evidence for a dopaminergic sexual dimorphism.** *Brain Res* (1985) **330**:55-64.

97. Spitz F, Demignon J, Porteu A, Kahn A, Concordet JP, Daegelen D, Maire P: **Expression of myogenin during embryogenesis is controlled by six/sine oculis homeoproteins through a conserved mef3 binding site.** *Proc Natl Acad Sci USA* (1998) **95**:14220-14225.

98. Stanfield B, Cowan WM: **Evidence for a change in the retino-hypothalamic projection in the rat following early removal of one eye.** *Brain Res* (1976) **104**:129-136.

99. Stephan FK, Zucker I: **Circadian rhythms in drinking behavior and locomotor activity of rats are eliminated by hypothalamic lesions.** *Proc Natl Acad Sci USA* (1972) **69**:1583-1586.

100. Storch KF, Paz C, Signorovitch J, Raviola E, Pawlyk B, Li T, Weitz CJ: **Intrinsic circadian clock of the mammalian retina: Importance for retinal processing of visual information.** *Cell* (2007) **130**:730-741.

101. Tronche F, Kellendonk C, Kretz O, Gass P, Anlag K, Orban PC, Bock R, Klein R, Schutz G: **Disruption of the glucocorticoid receptor gene in the nervous system results in reduced anxiety.** *Nat Genet* (1999) **23**:99-103.

102. Tucker P, Laemle L, Munson A, Kanekar S, Oliver ER, Brown N, Schlecht H, Vetter M, Glaser T: **The eyeless mouse mutation (ey1) removes an alternative start codon from the rx/rax homeobox gene.** *Genesis* (2001) **31**:43-53.

103. Turek FW: **Editor's introduction: The suprachiasmatic nucleus as the location of the master circadian pacemaker in mammals--significance for history of the field.** *J Biol Rhythms* (1996) **11**:283.

104. Ueda HR, Hayashi S, Chen W, Sano M, Machida M, Shigeyoshi Y, Iino M, Hashimoto S: **System-level identification of transcriptional circuits underlying mammalian circadian clocks.** *Nat Genet* (2005) **37**:187-192.

105. van der Horst GT, Muijtjens M, Kobayashi K, Takano R, Kanno S, Takao M, de Wit J, Verkerk A, Eker AP, van Leenen D, Buijs R *et al*: **Mammalian cry1 and cry2 are essential for maintenance of circadian rhythms.** *Nature* (1999) **398**:627-630.

106. Vandesompele J, De Preter K, Pattyn F, Poppe B, Van Roy N, De Paepe A, Speleman F: **Accurate normalization of real-time quantitative rt-pcr data by geometric averaging of multiple internal control genes.** *Genome Biol* (2002) **3**:34.31-34.12.

107. VanDunk C, Hunter LA, Gray PA: **Development, maturation, and necessity of transcription factors in the mouse suprachiasmatic nucleus.** *J Neurosci* (2011) **31**:6457-6467.

108. Wetsel WC, Mellon PL, Weiner RI, Negro-Vilar A: **Metabolism of pro-lhrh in immortalized hypothalamic neurons.** *Endocrinology* (1991) **129**:1584-1595.

109. Wetsel WC, Valenca MM, Merchenthaler I, Liposits Z, Lopez FJ, Weiner RI, Mellon PL, Negro-Vilar A: **Intrinsic pulsatile secretory activity of immortalized luteinizing hormone-releasing hormone-secreting neurons.** *Proc Natl Acad Sci U S A* (1992) **89**:4149-4153.

110. Wiegand SJ, Terasawa E: **Discrete lesions reveal functional heterogeneity of suprachiasmatic structures in regulation of gonadotropin secretion in the female rat.** *Neuroendocrinology* (1982) **34**:395-404.

111. Wierman ME, Xiong X, Kepa JK, Spaulding AJ, Jacobsen BM, Fang Z, Nilaver G, Ojeda SR: **Repression of gonadotropin-releasing hormone promoter activity by the pou homeodomain transcription factor scip/oct-6/tst-1: A regulatory mechanism of phenotype expression?** *Mol Cell Biol* (1997) **17**:1652-1665.

112. Wolfe A, Kim HH, Tobet S, Stafford DE, Radovick S: **Identification of a discrete promoter region of the human gnrh gene that is sufficient for directing neuron-specific expression: A role for pou homeodomain transcription factors.** *Mol Endocrinol* (2002) **16**:435-449.

113. Wray S, Grant P, Gainer H: **Evidence that cells expressing luteinizing hormone-releasing hormone mrna in the mouse are derived from progenitor cells in the olfactory placode.** *Proc Natl Acad Sci USA* (1989) **86**:8132-8136.

114. Yoon H, Enquist LW, Dulac C: **Olfactory inputs to hypothalamic neurons controlling reproduction and fertility.** *Cell* (2005) **123**:669-682.

115. Zhu CC, Dyer MA, Uchikawa M, Kondoh H, Lagutin OV, Oliver G: **Six3-mediated auto repression and eye development requires its interaction**

with members of the groucho-related family of co-repressors. *Development* (2002) **129**:2835-2849.